The natural history of luck: A synthesis study of structured population models

Christina M. Hernández *[a], Stephen P. Ellner[a], Robin E. Snyder[b] and Giles Hooker[c]

[a]Department of Ecology and Evolutionary Biology, Cornell University, Ithaca, New York.
[b]Department of Biology, Case Western Reserve University, Cleveland, Ohio.
[c]Department of Statistics and Data Science, Cornell University, Ithaca, New York.

Last compile: Nov 6, 2023

For submission at Ecology Letters, article type: **Synthesis**

Running title: The natural history of luck

Keywords: life history, luck, individual stochasticity, pace of life, reproductive skew, lifetime reproductive output, longevity, matrix population model, integral projection model, traits

Article components Abstract: **200** words; Main Text: **7491** words; 56 references; 6 figures in main text; 0 tables; 0 text boxes

Authorship statement: All authors contributed to conceiving the project. CMH did most of the coding, with input from RES and SPE. CMH performed analyses and visualization, and wrote most of the first draft. All authors discussed all aspects of the research, and contributed to the writing of the submitted manuscript.

Data availability statement: The data that support the findings of this study are openly available in Zenodo at http://doi.org/10.5281/zenodo.8199887.

*Corresponding author. Current address: Department of Biology, Oxford University, Oxford, United Kingdom. chrissy.hernandez@biology.ox.ac.uk

1 Abstract

Chance pervades life. In turn, life histories are described by probabilities (*e.g.*, survival, breeding) and averages across individuals (*e.g.*, mean growth rate, age at maturity). In this study, we explored patterns of luck in lifetime outcomes by analyzing structured population models for a wide array of plant and animal species. We calculated four response variables: variance and skewness in both lifespan and lifetime reproductive output (LRO), and partitioned them into contributions from different forms of luck. We examined relationships among response variables and a variety of life history traits. We found that variance in lifespan and variance in LRO were positively correlated across taxa, but that variance and skewness were negatively correlated for both lifespan and LRO. The most important life history trait was longevity, which shaped variance and skew in LRO through its effects on variance in lifespan. We found that luck in survival, growth, and fecundity all contributed to variance in LRO, but skew in LRO was overwhelmingly due to survival luck. Rapidly growing populations have larger variances in LRO and lifespan than shrinking populations. Our results indicate that luck-induced genetic drift may be most severe in recovering populations of species with long mature lifespan and high iteroparity.

2 Introduction

Luck shapes the outcomes of our lives in many ways. Think of all the events that had to occur exactly as they did for you to be reading this paper right now. In biology, some sources of randomness or unpredictability will persist no matter how many covariates we observe (Dietze, 2017). For example, whether a particular seed (among many near-identical seeds produced by one plant) lands on a rock or on the immediately adjacent soil is not due to any intrinsic property of that seed. But whether the seed germinates or perishes is determined by the chance event of landing in suitable or unsuitable habitat. The life history of an individual, *i.e.*, the schedule of their growth, reproduction, and death, involves a large sequence of chance events.

Within natural populations, individuals often vary substantially in their success, as measured by their lifespan or lifetime reproductive output. Many taxa, such as fish and trees, experience high mortality in early life and low mortality at larger sizes (Houde, 1989; Pauly, 1980; Van Valen, 1975). This mortality schedule causes high variance and skew in lifespan: most individuals die young, while some lucky individuals live a long time. High reproductive skew, where a small number of adults contribute the vast majority of reproductive output, is also common (Eusemann and Liesebach, 2021; Gerzabek et al., 2017; Goodwin et al., 2016; Le Boeuf et al., 2019; Ross et al., 2023). An important question in ecology is whether variation in success among individuals is due to their intrinsic properties or chance events.

Individuals differ in ways that impact survival, growth, and fertility, and thus lead to variation in lifespan or lifetime reproductive output. For example, populations are mixtures of individuals with various sizes, ages, phenotypes, and microhabitats. Size is particularly important in determining demographic rates because of its impacts on metabolism (Maino et al., 2014; West et al., 1997), fecundity (Allainé et al., 1987; Hixon et al., 2014; Weiner et al., 2009), predation risk (Juanes and Conover, 1994), and competition (De Roos et al., 2003). Fixed phenotypic traits can also have large impacts on demographic rates and lifetime success. In a population composed of both migratory and resident brown trout, migratory individuals produced the majority of offspring, despite being a minority of the adult population (Goodwin et al., 2016). Early-flowering forbs tend to produce more fruits and/or seeds (Munguía-Rosas et al., 2011), while canopy position strongly influenced seedling production in a population of similarly-sized oaks (Eusemann and Liesebach, 2021).

The study of 'luck', also referred to as 'individual stochasticity,' has focused on understanding the drivers of variation in success among individuals in the same population. These studies are generally based on structured population models (*i.e.*, matrix population models (Caswell, 2001) and integral projection models (Ellner et al., 2016)). In structured population models, individuals having the same state, such as size or age, are subject to the same probabilities of survival, growth, and reproduction. 'Luck' or 'individual stochasticity' arises because such individuals nonetheless

experience different outcomes: some live while others die, some have more offspring and some fewer, based on their state-dependent probabilities. We refer to lifespan and lifetime reproductive output as *lifetime outcomes* because they are the net result of many events over an individual's life.

Across populations, variation in demographic rates is directly linked to variation in life history traits. For example, high versus low mortality entails short versus long expected lifespan. Life history traits can generally be separated into traits relating to the pace of life (lifespan, age of maturity, fast vs. slow growth), and those that relating to reproductive investment (degree of iteroparity, clutch size) (Healy et al., 2019; Salguero-Gómez et al., 2016). Because demographic rates impact both life history traits and luck, we would expect the role of luck in a population to be strongly related to the population's life history traits. For example, individuals with a short lifespan will tend to have fewer reproductive events than individuals with a long lifespan. With all else held equal, a population with a shorter expected lifespan would show less variance in lifetime reproductive output. However, life history traits do not vary independently from one another, but are often constrained by trade-offs: when individuals invest in early reproduction or large clutch sizes, they tend to reach a smaller terminal size and have a shorter lifespan (Stearns, 1989). The non-independence of life history traits makes it difficult to predict which life history traits will most strongly drive variance in lifespan or lifetime reproductive output.

There is now a substantial literature focused on decomposing the variance across a population in individual lifetime outcomes into contributions from different sources. For example, a number of studies have examined models that include both individual age/size and a static phenotypic trait (*e.g.*, birth state, breeding strategy), and have found that the within-group variance (due to "luck" or "individual stochasticity") is often much larger than the between-group variance (due to "traits" or "individual heterogeneity") (Jenouvrier et al., 2022; Snyder and Ellner, 2018; Snyder et al., 2021; van Daalen et al., 2022). Age-partitioning of luck has shown that the conditions in early life, such as the birth state and early life survival and growth, are very important to determining an individual's lifetime outcomes (Snyder et al., 2021). Further work partitioning variance in lifetime reproductive output into contributions from various forms of demographic and environmental luck found that luck in survival, growth, or environmental variation dominated, depending on the life history traits of the population (Snyder and Ellner, 2022). Exciting recent mathematical progress enables the calculation of the full distribution of lifespan or lifetime reproductive output, suggesting that lifetime outcomes may frequently be bimodal (Tuljapurkar et al., 2020).

These previous studies have focused in depth on a few well-studied populations. Here, we complement those studies by taking a broad comparative approach to investigate patterns of luck across diverse plant and animal taxa. A comparative approach at this scale required us to focus on summary measures that describe the effects of luck in each population, and the important differences

among the populations, rather than a detailed examination of the full distributions of lifetime outcomes in particular populations (Tuljapurkar et al., 2020). Comparing across populations also required us to re-scale reproductive output so that we could compare apples to elephants. We do this by weighting offspring by their probability of surviving to a mature age, stage or size.

To describe the role of luck in populations, we focused on two summary measures of the distribution: variance and skewness, for two important lifetime outcomes: lifespan and lifetime reproductive output (LRO). To describe differences among populations, we used life history traits. We ask the following questions: (1) How do luck in lifespan and luck in LRO relate to each other? (2) Does high variance in a lifetime outcome predict high skewness in the same outcome— in other words, are variance and skewness equally useful as measures of inequality in lifespan and LRO? (3) How do life history traits relate to variance and skewness of lifetime outcomes? (4) How do different types of luck (survival, growth, fecundity) contribute to overall variance and skewness of lifetime outcomes?

We investigated these questions using a large set of structured population models from the COMADRE, COMPADRE, and Padrino databases (Levin et al., 2022; Salguero-Gómez et al., 2016; Salguero-Gómez et al., 2015). We calculated total variance and total skewness in both lifespan and lifetime reproductive output for each model, giving us four "response variables" of interest. We looked for relationships among the response variables, as well as relationships between each response variable and various covariates. The covariates included life history traits and model characteristics. We also decomposed the total variance and total skewness in lifespan and LRO into the contributions from luck in birth state, survival trajectory, growth trajectory, and fecundity. These decompositions were also tested for correlations with life history traits and model characteristics.

3 Selecting population models

To explore patterns of luck in lifespan and LRO across populations and taxa, we selected a large set of structured population models from the COMADRE (Salguero-Gómez et al., 2016) and COMPADRE (Salguero-Gómez et al., 2015) databases of matrix population models, and the Padrino database (Levin et al., 2022) of integral projection models. Our requirements were similar for matrix and integral models, but because matrix models predominate, we will explain our screening of COMADRE and COMPADRE and then mention a few items specific to Padrino.

To calculate our luck measures, survival and reproductive transitions must be quantified and separable in the model. For each model, we extracted the $\mathbf{F}$ and $\mathbf{U}$ matrices: the $\mathbf{F}$ matrix contains all of the reproductive transition rates, and $\mathbf{U}$ contains all of the survival and growth transition rates. The overall projection matrix for a population, $\mathbf{A}$, is the sum of $\mathbf{U}$ and $\mathbf{F}$.

We filtered for models that met basic quality control requirements such as no missing values and

no spontaneous production of individuals (*i.e.*, a column sum >1 in **U**). We required **A** matrices be ergodic, irreducible, and primitive. We excluded models that included clonal reproduction, two-sex models, and those that did not exhibit any reproduction. We included studies with any projection interval, and adjusted the time units in all calculated measures (*e.g.* lifespan, variance in lifespan, generation time, etc.) to years.

We filtered for models that were built from data in "Unmanipulated" conditions, and only models built from an individual population or pooled data from multiple populations (*i.e.*, we exclude models that are an element-wise mean of other matrix models). We also restricted our dataset to models with a population growth rate (λ) between 0.5 and 1.5, because extreme λ values can arise in laboratory conditions or can be an indication of data quality issues.

We corrected or removed from our study models with impossible life histories. Specifically, identified models with nearly 100% survival in the oldest size classes, which leads to "apparent immortality." We applied a correction to the survival matrices of these models following Hernández et al. (2023). If the final column sum of **U** was greater than 0.99, we attempted to scale it down to match another matrix from the same study/species, assuming that the unrealistically high survival probability was due to insufficient sample size in the largest size class. Amongst animal matrices, we were able to correct all 10 matrices with "apparent immortality." Among the 2367 plant matrices available at this point in the screening, there were 590 with this issue; 193 of those could not be corrected (and therefore were dropped) because no matrix from that study/species had a final column sum less than 0.99.

Because many of the calculations require the fundamental matrix ($\mathbf{N} = (\mathbf{I} - \mathbf{U})^{-1}$), we dropped an additional eight plant models for which (**I**-**U**) was singular after any **U** corrections as described above.

Finally, we manually screened for errors in representing the life cycle, following the issues identified in Kendall et al. (2019). In pre-breeding designs, we checked that survival of offspring over the first time step is accounted for in fertility rates. In post-breeding designs, we checked that survival of adults is accounted for in fertility transitions, and also checked that the matrix does not cause a reproductive delay (in other words, juvenile individuals reproduce in the first time step that they become mature). In the few models which used birth-flow designs, we checked that fertility rates accounted for newborn survival until age 0.5 (because the average offspring is 0.5 time steps old at the time of the census).

For integral projection models, the additional considerations were to include only deterministic, density-independent models for which the projection kernel K is a simple sum of a fertility kernel F and a survival-growth kernel P. Unrealistic survival leading to "apparent immortality" was also an issue with some of the integral projection models, but the required correction is different from

matrix population models. We took the column sum of the P kernel as the survival probability for the discretized size bins. Because IPM kernels are generally built outside of the range of observed individuals, we restricted our requirement of survival values to the range of size bins (1:k) corresponding to 99% of the stable age/size distribution. If there were any size bins in the 1:k range that had a survival probability greater than 0.99, then we rejected the model as being poorly fit (generally these are based on logistic regression with an asymptote at 1). If the survival probability was less than 0.99 for all size bins in 1:k, then we capped the probability of survival for any size bins larger than k to the probability of survival in size bin k.

After screening the databases according to our selection criteria, our data set consisted of 1489 structured population models. There were 462 models representing 80 animal species (450 matrix models and 12 integral projection models), and 1024 models representing 160 plant species (1017 matrix models and 7 integral projection models).

4 Calculations

We implemented integral projection models numerically using a bin-to-bin integration method, which is equivalent to a large matrix projection model. We therefore present our calculations in the notation and language of matrix projection models.

4.1 Moments of lifetime reproductive output and Lifespan

We calculated the mean, variance, and skewness of lifetime reproductive output using the framework of Markov Chains with rewards (Caswell, 2013; van Daalen and Caswell, 2017). In this framework, living individuals move through a set of transient states according to a matrix of state-dependent transition probabilities, and accrue rewards each time step according to the state- or transition-dependent probability distribution of reproductive output ("reward matrix"). Death is an absorbing state; dead individuals no longer change state and no longer accumulate rewards. The lifetime reproductive output of an individual is their total accumulated reward at the time of their death. van Daalen and Caswell (2017, Theorem 1) give formulas for the first, second, and third moments of LRO conditional on starting state, in terms of the first, second, and third moments of the reward matrix. We assumed that per-capita offspring production over one time step (*i.e.* "annual rewards"), conditional on an individual's state, was Poisson-distributed with the mean equal to the corresponding entry of the reproduction matrix (rescaled, see section 4.3 below). It is important to note that this assumption is applied only within individual states (*e.g.*, ages, sizes). The population-level distribution of clutch sizes depends on the distribution of individual states within the population, and need not follow a Poisson distribution. The equations that we used to

calculate mean, variance, and skewness of LRO are given in Appendix Section S1.

The mean, variance, and skewness of lifespan can be calculated as a special case where individuals accumulate exactly one unit of reward for each time step they are alive. The moments of lifespan conditional on starting state are given in Caswell (2013, Eqn. 21-23). The equations that we used to calculate mean, variance, and skewness of lifespan are given in Appendix Section S2.

4.2 Mixing distribution

In the calculations described so far, the mean, variance, and skewness are conditional on the starting state of an individual. For example, mean lifespan is calculated as a vector with entry L_i being the expected lifespan of an individual that starts life in state i. In an age-structured model, all individuals are born into the youngest age class. However, many of the models we analyzed are size- or stage-structured, and individuals can start in multiple states. In that case we must calculate the mean, variance, and skewness in lifespan by averaging over the possible starting states. This averaging is achieved by applying a mixing distribution for initial state and the law of total variance or total cumulance (see Appendix Section S1 for more details and equations).

We selected a standard mixing distribution, the distribution of offspring types in a cohort born at the stable population distribution:

$$\boldsymbol{\pi}_z = \frac{\mathbf{Fw}}{\|\mathbf{Fw}\|}, \tag{1}$$

where $\mathbf{w}$ is the dominant right eigenvector of the population projection matrix ($\mathbf{A}$). Note that $\boldsymbol{\pi}_z$ is also the probability of being born into each state, when the population is at its stable population distribution.[1]

4.3 Offspring weight function

To compare LRO measures across taxa, we defined an offspring weighting function that could normalize the 'units' of LRO. Not all offspring are worth the same amount: a seed in the seedbank is less likely to contribute to future population growth than is a seedling or first-year flowering offspring. Additionally, offspring are not worth the same across species, and cross-species comparisons will be affected by the propensity for some species to produce few offspring that mostly survive until adulthood while others produce many offspring with high juvenile mortality. To have consistent 'units' of LRO, we only 'count' the offspring that survive to adulthood. Rather than using the total stage-specific reproductive output as the stage-specific rewards, we used the sum of stage-specific offspring weighted by each offspring's probability of surviving to adulthood. For

[1]The next subsection describes our method for re-scaling the $\mathbf{F}$ matrix for cross-model and cross-taxa comparisons. Note that we do *not* re-scale the $\mathbf{F}$ matrix in the calculation of the mixing distribution. The mixing distribution is based on population structure and cohort distribution, while the rescaled $\mathbf{F}$ matrix is used *only* for calculating rewards (*i.e.*, moments of lifetime reproductive output).

example, adults that produce both seeds and seedlings will receive rewards with a smaller weight from the seeds than the seedlings. This weighting also has the advantage of compensating for the effect of pre- vs. post-reproductive census on LRO, *i.e.*, whether offspring are counted after or before first-year mortality.

We assumed that stage-specific offspring production was Poisson-distributed, with means given by the values in the fertility matrix ($\mathbf{F}$). From the probability mass function of the Poisson distribution, we derived the stage-specific probability of breeding (having more than 0 offspring) as:

$$\mathbf{p_b} = 1 - e^{-f_i}, \tag{2}$$

where f_i is the i-th column sum of $\mathbf{F}$. Note that $\mathbf{p_b}$ is a column vector with a probability of breeding for each starting state. We calculated the probability of surviving to reproduce at least once (*i.e.*, entering the breeding population, B), conditional on individual birth state (z_0), following Ellner et al. (2016, p. 67), as:

$$\mathbb{P}(B|z_0) = \mathbf{p_b^\mathsf{T} N_0}, \tag{3}$$

where $\mathbf{N_0}$ is the fundamental matrix for a modified state transition matrix where reproduction is an absorbing state. We generated the expected rewards matrix ($\mathbf{R}_1$) by multiplying each nonzero entry F_{ij} by the i^{th} entry of Eqn. (3).

4.4 Decomposition of variance and skewness: Types of luck

To understand how different categories of luck drive overall variation in lifetime outcomes, we decomposed each of our four lifetime outcome measures into contributions from different categories of luck, using the approach of Snyder et al. (2021). *Birth state* luck is variation in outcomes resulting from individuals by chance having different states at birth (*e.g.*, different sizes). *Survival trajectory* luck is variation in outcomes resulting from the fact that each year, among individuals with the same state and therefore the same mortality risk, by chance some will live and some will die. *Growth trajectory* luck is variation in outcomes due to the fact that individuals with the same state at any time t will by chance have different states at time $t + 1$. *Fecundity luck* (which only affects LRO measures) is variation in LRO due to chance differences in actual annual offspring production among individuals who have the same sequence of state transitions from birth to death.

Elsewhere we have derived methods to calculate sequentially the expected contribution of each type of luck at each age of life to the lifetime reproductive variance and skewness (Snyder and Ellner, 2023; Snyder et al., 2021). The idea behind the approach is that learning the actual outcome of one more event in an individual's life (rather than knowing just the range of possible outcomes and their probabilities) changes the distribution of the outcome measure conditional on everything that

has happened so far in the individual's life. For example, knowing that an individual survived from age 4 to age 5 in an age-structured model changes the conditional mean of LRO: from the mean conditional on survival, growth, and reproduction up to age 4, to the mean conditional on all of those things plus survival to age 5. The amount of change by the inclusion of an additional stage transition measures the importance of survival luck at age 4 for that outcome measure. Snyder et al. (2021, pp. E112 - E117) derived explicit formulas for all such age-specific contributions to LRO and lifespan variance, for any density-independent matrix or integral projection model, and have extended those calculations to skewness (Snyder and Ellner, 2023). Here we only consider the total contribution of each type of luck, calculated by summing each type over all ages. To ensure that the sum over all ages includes all possible life histories, we set the maximum age in the sum to 300 years for animals, and 5000 years for plants.

4.5 Model structure and life history traits

We investigated how life history traits and model structure covariates impact luck by exploring relationships of our four luck measures with six life history traits and three model characteristics. For model characteristics, we looked at (1) population growth rate (λ, the leading eigenvalue of the projection matrix or kernel); (2) the number of stages in the model (for matrix population models only), and (3) taxonomic class (animals) or organismal growth form (plants).

We selected life history traits that can be calculated directly from the population projection matrix (or kernel). We calculated three traits related to the pace of life: longevity, expected age at first reproduction, and generation time. We also calculated three traits related to reproductive strategy: precocity, iteroparity, and average clutch size.

Longevity We define longevity as the expected total lifespan of adults (individuals that reproduce at least once) rather than the expected lifespan of all individuals, in order to avoid sensitivity to early life processes. When early life mortality is very high, expected lifespan will be quite low even if a typical adult lives a long time. For example, in bluefin tuna, adults are known to reach ages of ~ 40 years, but early life mortality is over 99% and most individuals die very young. For brevity, we will refer to *the expected lifespan of individuals who reproduce at least once* as "longevity" from here on.

We computed longevity from an expanded Markov chain with two absorbing states: dead with

lifetime reproductive output equal to zero (Ω_1) or greater than zero (Ω_2):

$$\mathbf{P} = \left(\begin{array}{c|c|cc} \mathbf{T}_{\tau\times\tau} & \mathbf{0}_{\tau\times\tau} & \mathbf{0}_{\tau\times 1} & \mathbf{0}_{\tau\times 1} \\ \hline \mathbf{R}_{\tau\times\tau} & \mathbf{U}_{\tau\times\tau} & \mathbf{0}_{\tau\times 1} & \mathbf{0}_{\tau\times 1} \\ \hline \mathbf{M}_{1\times\tau} & \mathbf{0}_{1\times\tau} & 1 & 0 \\ \mathbf{0}_{1\times\tau} & \mathbf{M}_{1\times\tau} & 0 & 1 \end{array}\right), \tag{4}$$

where $\mathbf{T}$ contains the transition probabilities for surviving and not reproducing, $\mathbf{R}$ contains the transition probabilities for surviving and reproducing, and $\mathbf{U}$ contains total survival probabilities, as usual. The mortality vector $\mathbf{M}$ contains the state-dependent probability of death, which is not affected by past reproductive output.

Longevity is calculated as the expected time to absorption conditional on absorbtion into Ω_2. Using standard Markov chain methods we calculated the transition matrix (4) conditional on absorbtion into Ω_2 and the mean time to absorbtion for that matrix (see *e.g.*, Snyder and Ellner (2016)). The full set of equations is provided in Appendix Section S3.

Age of maturity We calculated the age of maturity as the expected age at which an individual will first reproduce (Cochran and Ellner, 1992). Specifically, we calculated the expected lifespan in a modified Markov Chain where individuals are 'absorbed' when they first reproduce (Caswell, 2001, Section 5.3.3).

Generation time We selected T_a as the measure of generation time, the time between successive birth events in the ancestral genealogy of an individual (Bienvenu and Legendre, 2015). This measure is equivalent to $\bar{A}$ as presented in Cochran and Ellner (1992), which is the mean age of parents of a cohort of offspring produced at the stable stage distribution (Bienvenu and Legendre, 2015). In stationary populations ($\lambda = 1$), T_a will also be equivalent to the mean age at lifetime birth events across a cohort of newborns at the stable stage distribution with offspring weighted by reproductive value ($\mu_1(v)$; Ellner 2018). When survival is very high in the oldest/largest classes and the population is growing quickly, we expect T_a to be much less than $\mu_1(v)$. Although individuals continue reproducing until very old ages (driving $\mu_1(v)$ up), the typical offspring being produced 'now' has a young parent (driving T_a down) because a rapidly growing population will have a stable stage distribution skewed towards young individuals. Therefore, we selected T_a because it more closely represents what we *mean* when we say 'generation time.' It is calculated as:

$$T_a = \frac{\lambda \mathbf{v}^\mathsf{T}\mathbf{w}}{\mathbf{v}^\mathsf{T}\mathbf{F}\mathbf{w}}, . \tag{5}$$

where $\mathbf{w}$ and $\mathbf{v}$ are the left and right eigenvectors corresponding to λ. These eigenvectors also represent the stable stage distribution ($\mathbf{w}$) and reproductive value ($\mathbf{v}$).

We found that, for some models, T_a gives unreasonably high values (thousands of years in some herbaceous perennials, hundreds of years in some marine invertebrates) even if the model seems otherwise reasonable. Inspecting these models, it seems that the extremely high values of T_a are due to reproductive value ($\mathbf{v}$) that peaks at the oldest/largest individuals, which in turn seems to be more likely to occur if retrogression is common.

Precocity We defined precocity as one minus the ratio of mean age at first reproduction to mean lifespan for reproductive individuals. A precocity score close to one indicates early-life maturity, while a precocity score close to 0 indicates late-life maturity.

Iteroparity We calculated iteroparity from Demetrius' evolutionary entropy (Demetrius, 1977; Demetrius et al., 2009), using the `Rage` package (Jones et al., 2022). Iteroparity scores <1 indicate individuals are approximately semelparous, while high values indicate that individuals experience many reproductive events in their lifetime.

Average clutch size We defined average clutch size as the per capita offspring production by adults at the stable stage distribution:

$$F_{clutch} = \frac{\mathbf{Fw}}{\sum_a \mathbf{w}}, \tag{6}$$

where the denominator is the sum of the portion of the stable stage distribution that is reproductively active (a indicates the adult stages).

5 Results and Interpretation

5.1 Relationships among the response variables

We primarily used Kendall's nonparametric correlation coefficient τ to quantify and statistically test for relationships among variables, because of the highly non-normal distribution of variables.

Variance Lifespan variance and LRO variance were positively correlated (Figure 1A,B) for both animals ($\tau = 0.460, p < 0.001$) and plants ($\tau = 0.224, p < 0.001$). This matched our expectations, because the number of reproductive events should increase with lifespan, and the variance of any measure will generally increase with the mean. Greater variance in lifespan should therefore lead to greater variance in the number of reproductive events which, in turn, should generally increase the variance in LRO. Although the slope of the relationship varied slightly among the well-represented

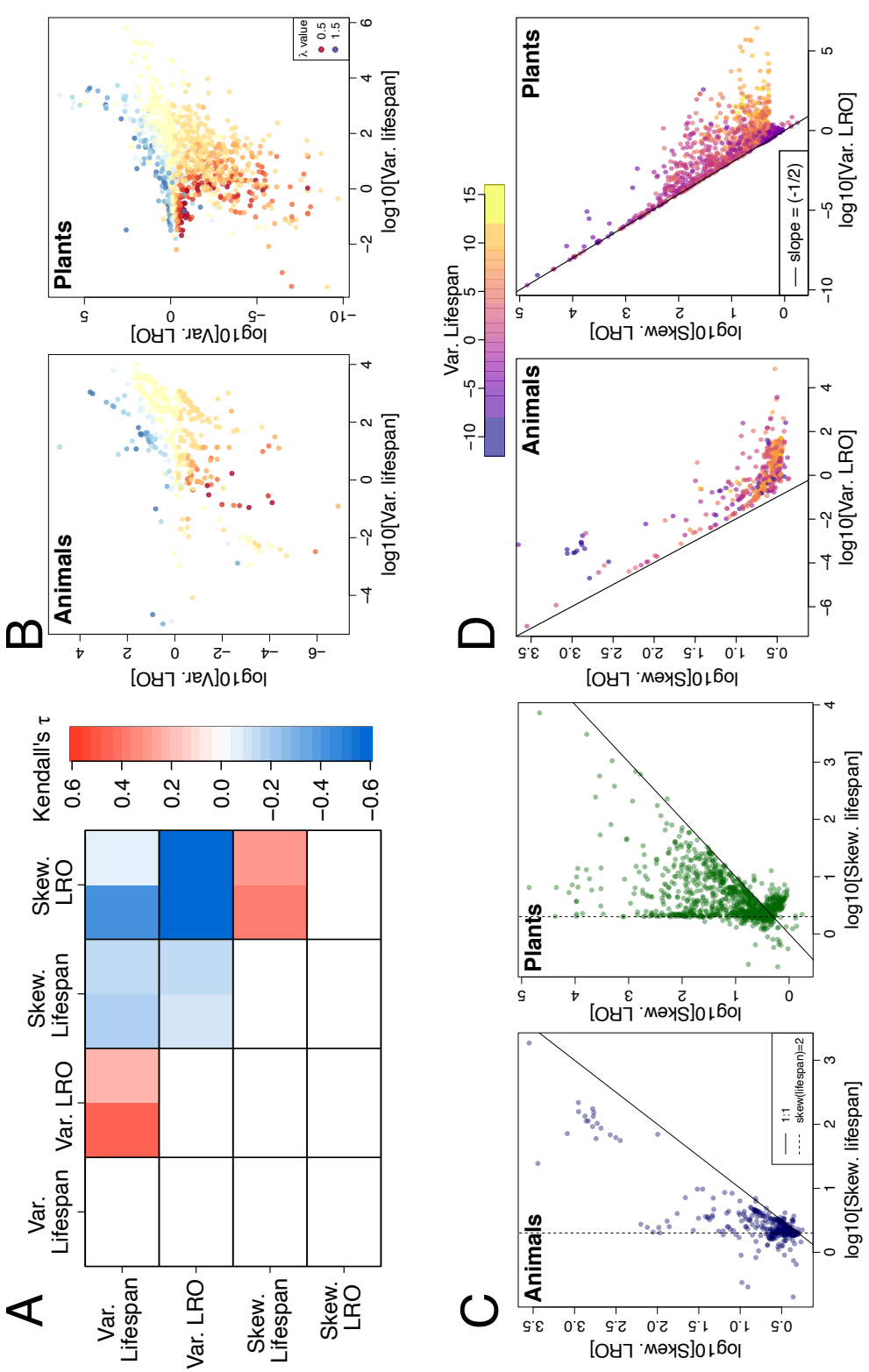

Figure 1: (Caption next page.)

Figure 1: (Previous page.) Relationships among response variables are strong and consistent across animals and plants. (A) Kendall's τ estimates for pairwise relationships among the response variables: variance in lifespan, variance in LRO, skewness of lifespan, and skewness of LRO. Entries along the diagonal (correlation of a variable with itself) and the repeated pairwise relationships in the lower triangular region are blocked out in white. Within each square, the estimate of τ is shown for animals on the left and plants on the right. All pairwise τ estimates were statistically significant ($p < 0.05$). The additional panels show (B) the relationship between lifespan variance and LRO variance colored according to λ; (C) the relationship between lifespan skewness and LRO skewness; and (D) the relationship between variance and skewness of LRO colored according to lifespan variance. In panels B-D, each point represents one population model (*i.e.*, a particular parameterization of a matrix population model or integral projection model). In panels B-D, both axes are log-scaled. Note that log-transformed variance is equivalent to twice the log-transformed standard deviation [$\log(var(x)) = 2 * \log(sd(x))$].

taxonomic classes in animals and among growth forms in plants, the relationship was positive for all groups (Figure S1).

We were surprised to see that population growth rate (λ) structured the relationship between variance in lifespan and variance in LRO (Figure 1B). Shrinking populations ($\lambda < 1$) exhibited lower variance in both lifespan and LRO than growing populations ($\lambda > 1$). We investigated a few possible mechanisms that might explain this relationship, but none were supported (see the Discussion). We also observed that some of the microstructure, particularly for animals, was related to matrix size (Figure S2). Matrix size may be more meaningful in animal models, which were frequently age-structured, while nearly all plant models were size-structured.

Skewness Lifespan skewness and LRO skewness were also positively correlated (animals: $\tau = 0.39, p < 0.001$; plants: $\tau = 0.29, p < 0.001$). We expected this relationship because when lifespan is highly skewed, relatively few individuals survive long enough to reproduce. LRO skewness tended to be greater than lifespan skewness (most points above the 1:1 line, Figure 1C). The slope of the relationship was positive and similar across most taxonomic groups and growth forms, except for a very flat slope for mammals (Figure S3). Unlike variance, the skewness of lifespan and LRO did not show structuring with λ (Figure S4). Likewise, there was no obvious structuring with matrix dimension (Figure S5).

Most populations exhibited lifespan skewness ≥ 2 (Figure 1C). If survival rate is independent of age in a continuous-time model, lifespan would be exponentially distributed, having skewness of 2. In discrete time with constant survival probability, lifespan is geometrically distributed, and skewness varies between 2.31 and 2 for mean lifespans of 1.5 and above. Elevated juvenile mortality, so that many individuals die young but those that reach adulthood have roughly constant annual survival, produces skewness greater than 2.

Variance and Skewness Variance and skewness were negatively related for both lifespan and LRO (Figures 1A,D and S6). In populations with greater lifespan variance, the skewness of both lifespan and LRO was decreased. Likewise, in a population with greater variance in LRO, there was lower skewness of lifespan and LRO. The skew-variance relationship for LRO was bounded by a line with a log-log slope of $-1/2$ (Figure 1D), which is the relationship for Poisson distribution (skewness $= 1/\sqrt{\text{variance}}$). Under our assumptions, a population where all individuals reproduce exactly once (*e.g.*, biennials) would lie on this line. There are (at least) two mechanisms that would move populations to the right of the boundary line. First, a zero-inflated Poisson distribution exhibits higher skewness for a given variance. Second, the sum of a geometrically-distributed number of Poisson distributions (*i.e.*, repeated reproduction over a geometrically-distributed lifespan) exhibits higher skewness for a given value of variance. High variance in lifespan could be caused by both of these phenomena: zero-inflation due to individuals that die before reproducing, and geometrically-distributed numbers of reproductive events in long-lived adults. This suggests that LRO would become less Poisson-distributed with increased variance in lifespan, and this is what we saw (Figure 1D).

5.2 Relationships between response variables and life history traits

Life history traits Many of the life history traits we examined were positively correlated in pairwise comparisons: longevity, age of maturity, generation time, and iteroparity (Figure 2). Precocity showed weak positive relationships with longevity, iteroparity, and average clutch size. Lifespan sets the possible scope for many of the traits that we examined. For example, if longevity is short, then generation time must also be short. Likewise, high iteroparity requires a long lifespan,[2] and precocity was measured relative to the expected lifespan of reproductive individuals.

Larger average clutch size was associated with earlier maturity, shorter mature lifespan, shorter generation times, and less iteroparity. This is consistent with a life history trade-off between reproductive investment and adult survival.

Variance In both plants and animals, high lifespan variance was strongly associated with greater longevity (Figure 2). The life history traits that were positively correlated with longevity were also positively related to variance in lifespan (Figures 2, S7, and S8). Conversely, populations with high average clutch size tended to have low variance in lifespan.

Variance in LRO exhibited positive relationships for precocity, iteroparity, and clutch size (Figures 2 and S9). Precocity and iteroparity likely influence variance in LRO through their effects on

[2]This is not *necessarily* the case. A discrete-time model cannot give high iteroparity if individuals do not live for a large number of time steps. If the model time step were shorter, then a population could have a high iteroparity score and an expected lifespan much shorter than one year. However, most models in this study have a time step of one year or 5 years (in the case of long-lived trees and palms).

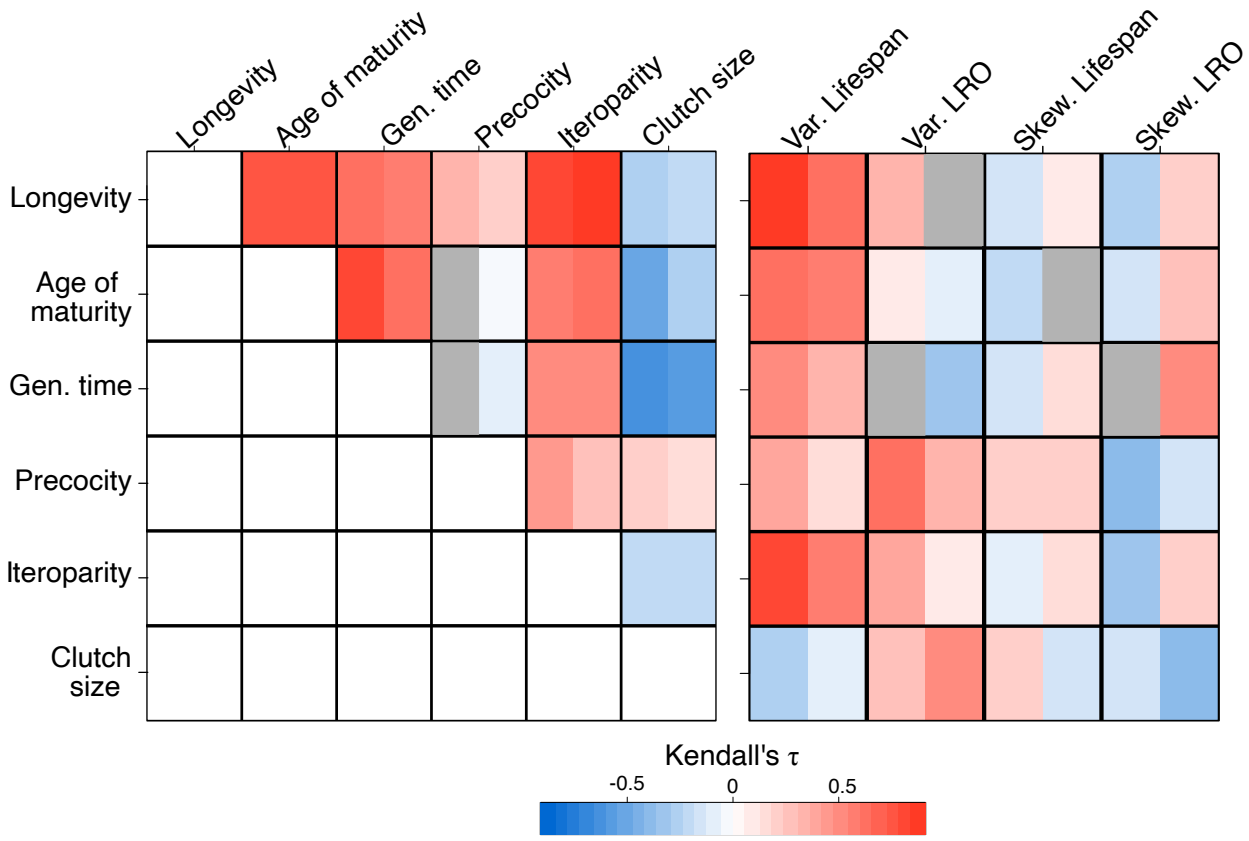

Figure 2: Plants and animals vary in the observed relationships between life history traits and response variables, despite consistent relationships among life history traits across kingdoms. (Left) τ estimates for relationships among life history traits and (Right) relationships between each of the response variables (variance in lifespan, variance in LRO, skewness of lifespan, and skewness of LRO) and life history traits. Within each square, the estimate of τ is shown for animals on the left and plants on the right. All depicted τ estimates are statistically significant ($p < 0.05$); grey fill indicates a non-significant relationship.

the mean and variance in the number of reproductive events that individuals experience (*i.e.*, the argument that we made above to explain why variance in lifespan and variance in LRO should be positively correlated). Higher average clutch size increased variance in LRO because we represented reproduction as a Poisson process (the Poisson distribution has variance equal to its mean).

Although variance in lifespan and variance in LRO were positively correlated, they did not always show the same relationships with life history processes. We expected variance in LRO to increase with greater longevity, but this was observed only in animals (no significant relationship was observed in plants). In fact, other traits that were positively related to longevity– late age of maturity and long generation time– were related to *decreased* variance in LRO for plants (Figures 2 and S10).

It is possible that the positive relationship between variance in LRO and average clutch size is enough to account for this surprising negative relationship of variance in LRO with generation time and age of maturity in plants. If average clutch size were the dominant driver of variance in LRO, then a negative relationship between variance in LRO and generation time could be the result of the negative relationship between average clutch size and generation time. As we argued above, the negative relationship between clutch size and generation time may be a consequence of life history trade-offs.

Skewness Skewness of lifespan generally exhibited weak relationships with the life history traits we considered (Figures 2 and S11-S14). Surprisingly, these relationships tended to be in the opposite directions for plants and animals: a larger clutch size was associated with greater skewness in lifespan in animals, but lower skewness in lifespan in plants. This difference may be related to a difference in the shape of survival curves between plants and animals. The animal models are dominated by mammals and birds which generally have much lower clutch sizes and higher early-life survival than plants. In fact, when we separated out fish, which tend to have survival schedules and clutch sizes more similar to plants than to birds, we found that fish have correlations in the opposite direction from the other animal populations, and in agreement with plants (Figure S15).

Because there was a strong negative relationship between variance and skewness in LRO, skewness and variance of LRO often related to life history traits in opposite ways. In animals, the five life history traits that showed significant positive relationships with LRO variance all show significant negative relationships with LRO skewness. In plants, all of the relationships flip sign as expected *except* for iteroparity, which shows a weak positive relationship with variance in LRO and a stronger positive relationship with skewness in LRO.

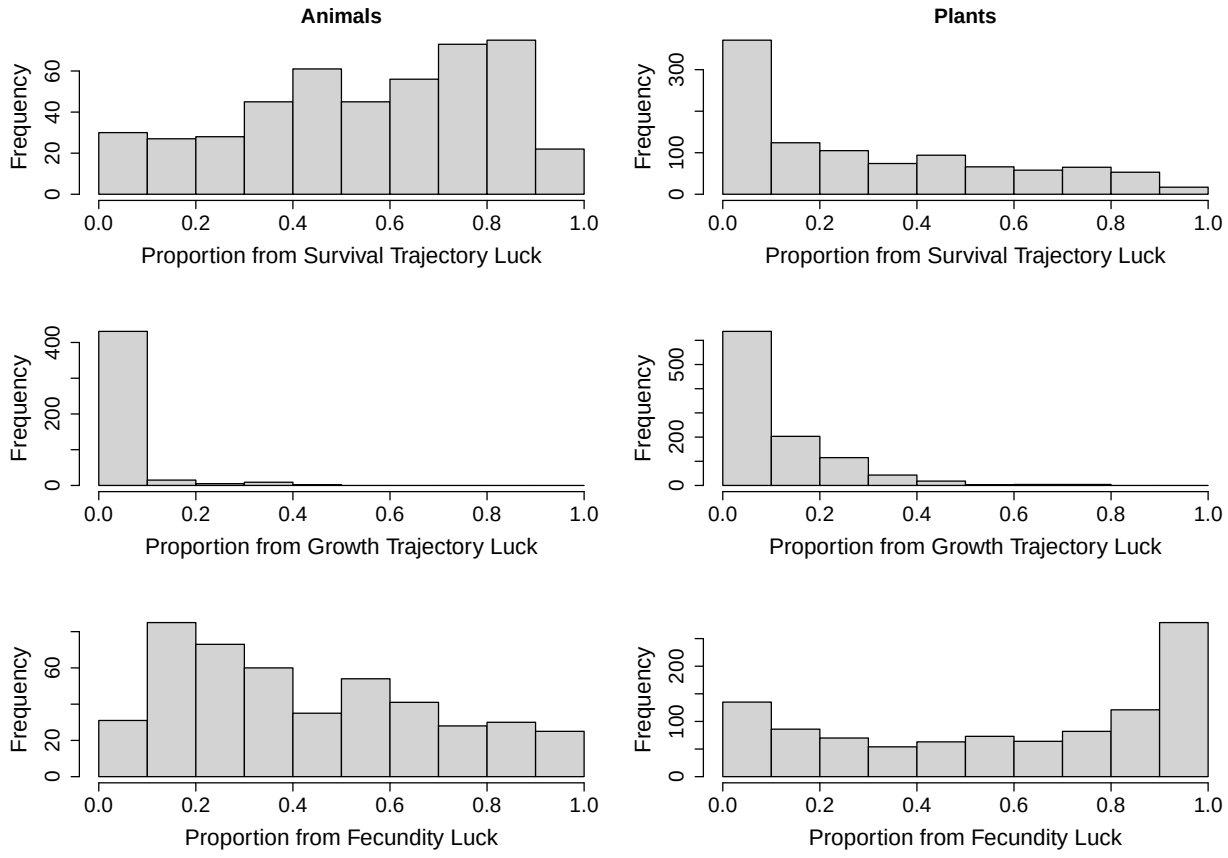

Figure 3: Variance in LRO is primarily driven by survival trajectory luck and fecundity luck, in both plants and animals. Decomposition of variance in LRO into proportional contributions from survival, growth, and fecundity luck. We do not show birth state here because it contributes less than 5% of the variance in LRO in all of the animal models, and in nearly all (95%) of the plant models.

5.3 Contributions of multiple types of luck to variance and skewness

Variance Variance in lifespan overwhelmingly tended to come from uncertainty in the survival trajectory in animals, with more contributions from the growth trajectory in plants (Figure S16). In an age-structured model, the "growth trajectory" is simply the deterministic process of becoming a year older with each time step, so there is no growth trajectory luck. Animal models are much more frequently age-structured while plant models are more usually size-structured, which accounts for the difference in the role of growth trajectory in determining variance in lifespan. Uncertainty in the birth state played a very small role, accounting for less than 3% of the variance in all animal models, and less than 5% of the variance in 95% of the plant models.

Variance in LRO was determined primarily by survival trajectory luck and fecundity luck (Figure 3). In animal models, which are mostly age-classified, survival trajectory luck tended to be more important than fecundity luck. In plant models, fecundity luck tended to be far more important than survival trajectory luck. The large role for fecundity luck is in part a consequence of the offspring weighting that we used. When we rescaled age-specific reproductive output (the $\mathbf{F}$ matrix) by an offspring's probability of surviving to reproduce at least once, the luck of survival or death during the pre-reproductive period was shifted from survival trajectory luck to to fecundity luck. For more mathematical details on how variance partitioning is impacted by rescaling $\mathbf{F}$, see Appendix Section S4.

The dominant component of variance in LRO showed a sharp shift between shrinking and growing populations in both animals (Figure 4A) and plants (Figure 5A). In shrinking populations ($\lambda < 1$), fecundity luck is the largest contributor to total variance in LRO. In growing populations ($\lambda > 1$), survival luck contributes the same amount or more than fecundity luck to total variance in LRO. This means that, in shrinking populations, individuals with particularly high LRO would tend to be those who have above-average clutch sizes. In growing populations, individuals with particularly high LRO would tend to be those that survive longer than average.

Skewness skewness in lifespan and LRO showed a markedly different pattern. The contributions from survival trajectory luck to skewness in lifespan are centered on 100%, and both growth trajectory luck and birth state luck are centered on 0 (Figure S17). For LRO, contributions from survival trajectory luck tended to account for more than 100% of the skewness while contributions from growth trajectory luck and fecundity luck were negative, decreasing the overall skewness of LRO (Figure 6).

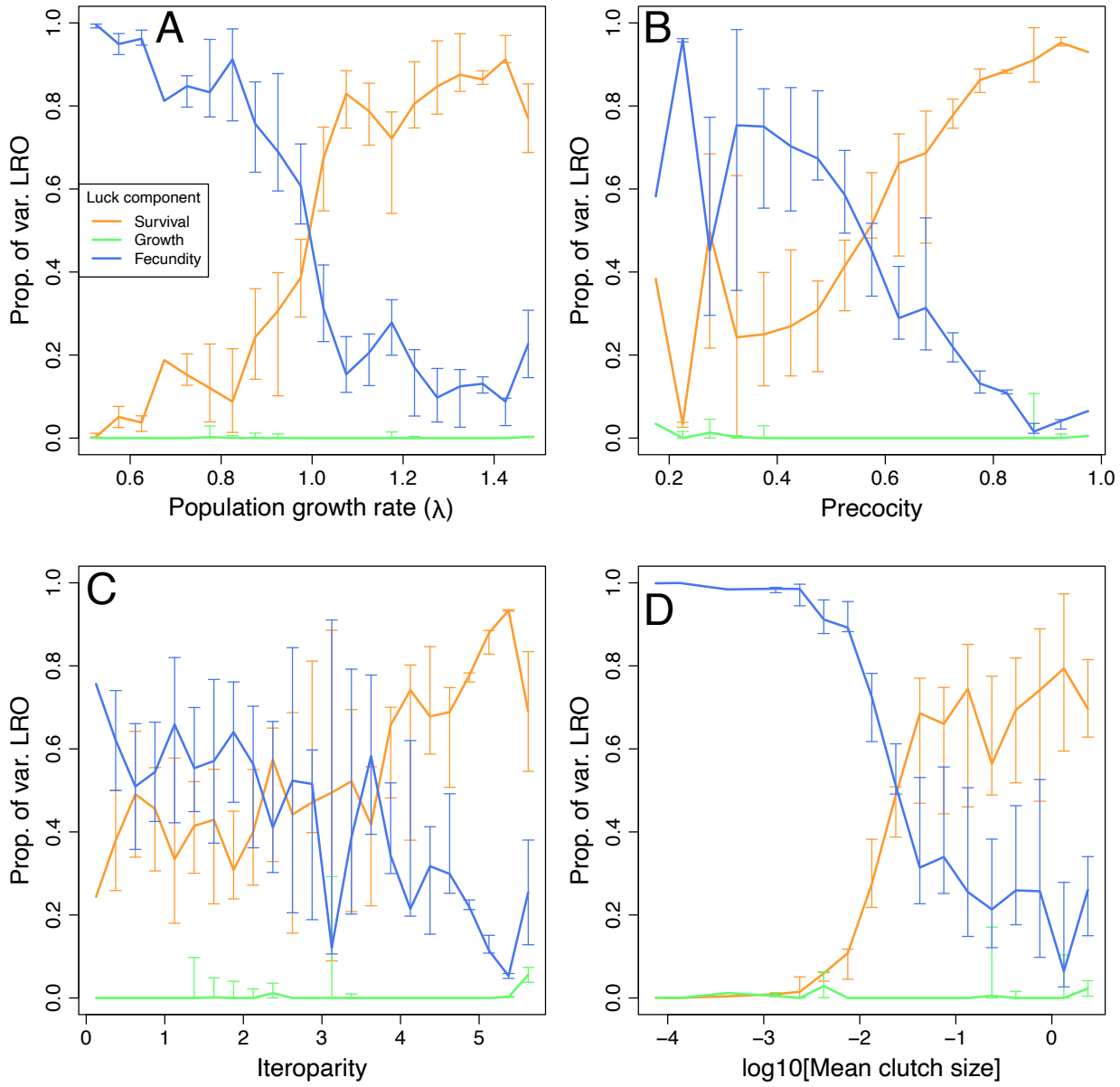

Figure 4: Population growth rate and reproductive strategy traits influence the proportion of variance in LRO due to survival vs. fecundity luck in animals. We plot the proportion proportion of total variance in LRO from survival trajectory luck, growth trajectory luck and fecundity luck for animals as a function of: (A) population growth rate λ, (B) precocity, (C) iteroparity, and (D) mean clutch size. For each sub-panel, data are grouped into 17-23 bins. Lines represent the median value in each bin, and the bars mark the 25% and 75% quantiles (plotted at each bin's midpoint).

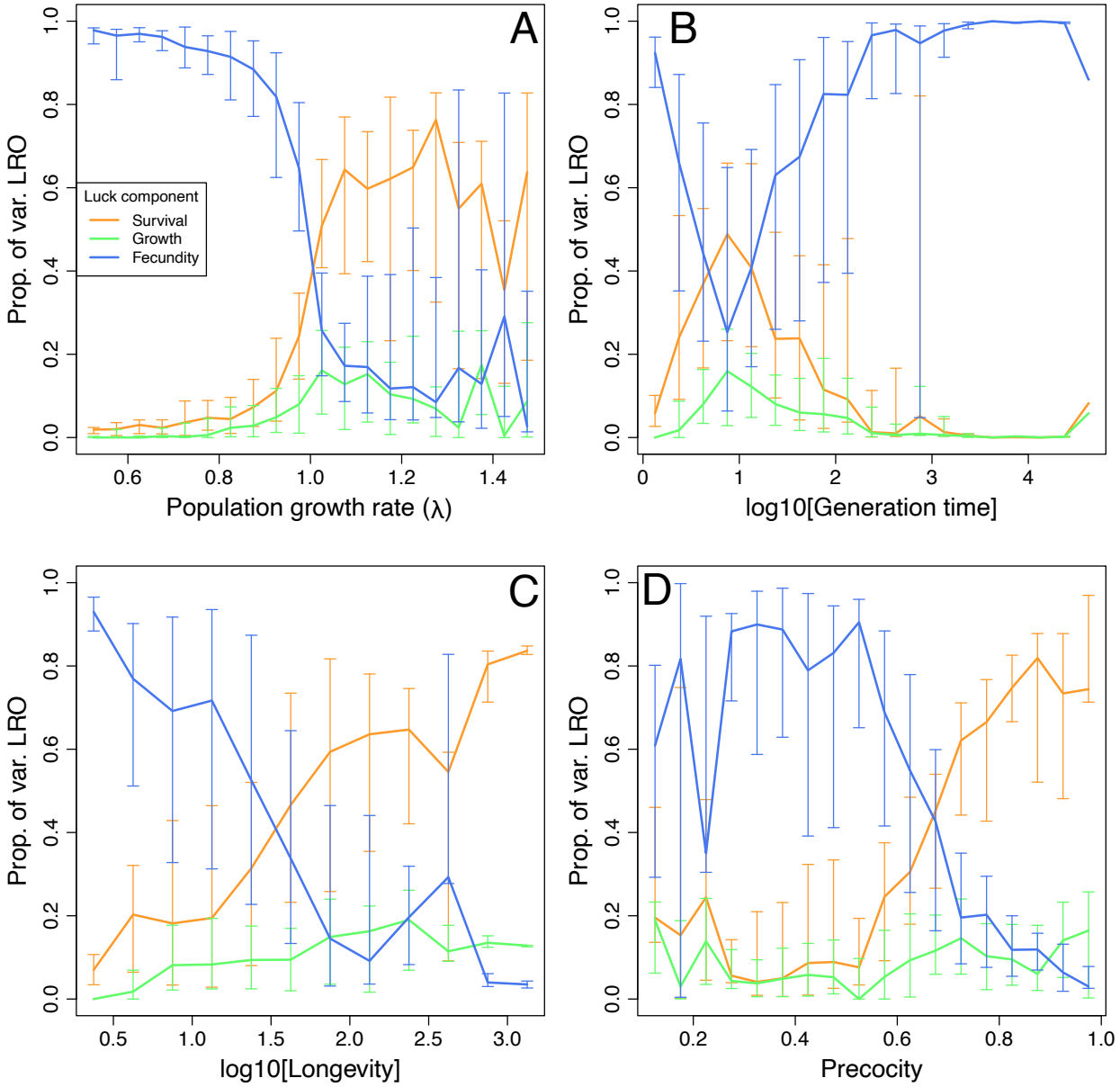

Figure 5: Population growth rate and pace-of-life traits influence the proportion of variance in LRO due to survival vs. fecundity luck in animals. We plot the proportion proportion of total variance in LRO from survival trajectory luck, growth trajectory luck and fecundity luck for animals as a function of: (A) population growth rate λ, (B) generation time, (C) longevity (lifespan of reproductive individuals), and (D) precocity. For each sub-panel, data are grouped into 12-20 bins. Lines represent the median value in each bin, and the bars mark the 25% and 75% quantiles (plotted at each bin's midpoint).

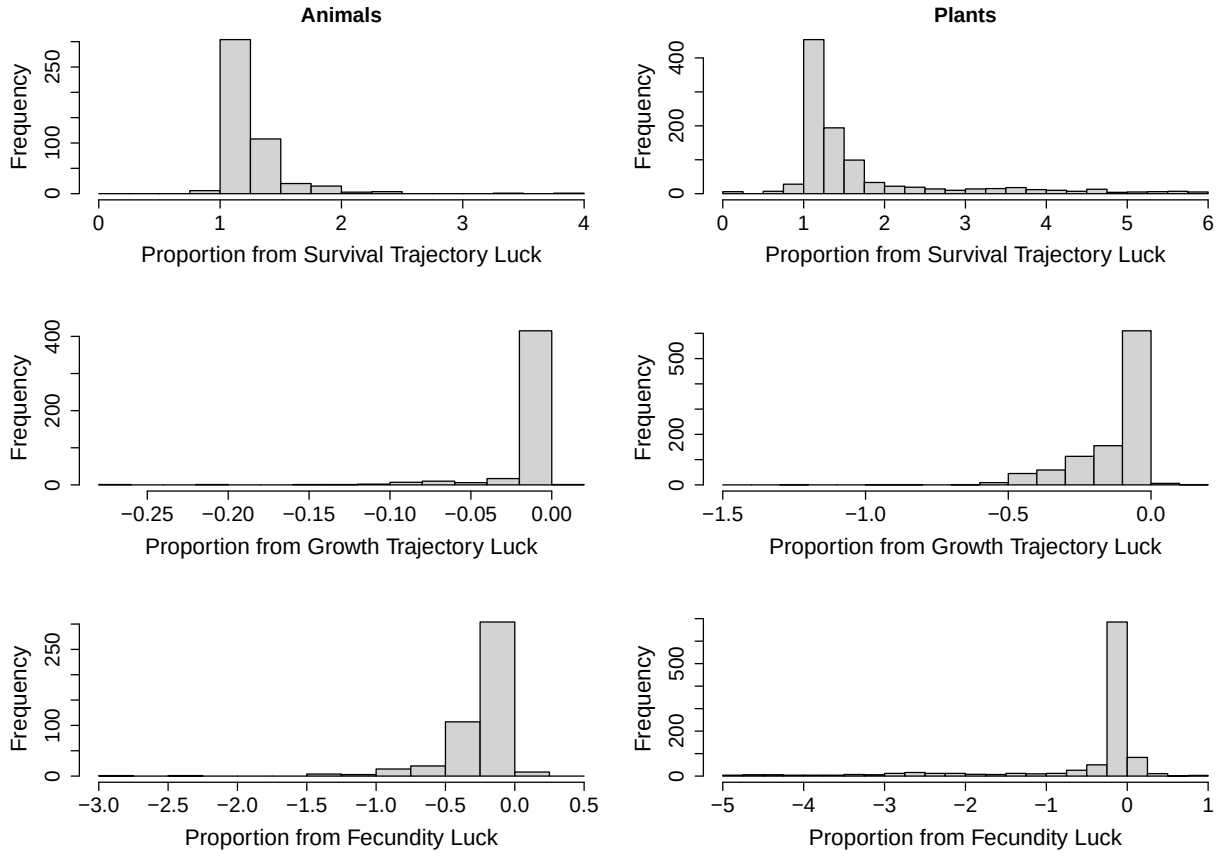

Figure 6: Skewness in LRO is overwhelmingly due to survival trajectory luck. Decomposition of skewness in LRO into contributions from survival, growth, and fecundity luck. We do not show birth state here because it contributes less than 1% of the variance in LRO in all of the animal models, and in nearly all (99.6%) of the plant models.

5.4 Life history traits and components of variance in LRO

Finally, we explored how life history traits influenced the proportional contributions to variance in LRO. We examined exploratory scatter plots (not shown), and discuss here only the life history traits that influenced the components of variance in LRO.

In animals, the proportion of variance in LRO due to fecundity luck vs. survival luck depended on reproductive strategy traits (Figure 4). As precocity, iteroparity, and mean clutch size increased, survival trajectory luck became more important in determining total variance in LRO. In highly precocious animals, nearly all individuals will survive to reproduce at least once, so the variance in LRO is generated by differences in individuals' survival trajectories. In populations with very low iteroparity, the typical individual reproduces only once, so fecundity luck dominates. And when average clutch size is large, a typical reproductive individual will have at least one offspring every year, so the survival trajectory is the main determinant of becoming a 'lucky' reproducer who contributes many offspring to the population.

In plants, variance in LRO showed important contributions from three kinds of luck: survival, growth, and fecundity. The proportion of variance in LRO contributed by growth luck did not change dramatically with different life history traits. Fecundity luck showed an increasing importance as generation time increased, but a decreasing importance as longevity increased. Survival luck tended to dominate the variance in LRO in populations with a long lifespan, while fecundity luck tended to dominate in populations with long generation time. Similar to the pattern in animals, the contribution of survival trajectory luck to the variance in LRO increased with greater precocity. Populations that are highly precocious may have high longevity (they start reproducing long before they die), and so differences in the survival trajectory separate individuals with high LRO from those with low LRO. Populations with extremely long generation time may be declining populations that are dominated by old individuals with high survival; in these populations, variation in fecundity primarily generates the variation in LRO.

6 Discussion

The study of "luck" in individual life histories in recent decades has been motivated in part by a desire to understand the drivers of reproductive skew, a frequently observed phenomenon wherein a small number of individuals produce most of the offspring. These exceptional or "lucky" individuals therefore contribute disproportionately to population maintenance and growth. Past studies (*e.g.*, Jenouvrier et al., 2022; Snyder and Ellner, 2016, 2018; van Daalen et al., 2022) have focused in detail on a limited number of well-parameterized populations to explore the drivers of variance and quantify the contributions from individual phenotypic traits ("individual heterogeneity") and luck

("individual stochasticity"). Here, we focused on models where individuals vary only in their age, size, or stage but without additional phenotypic variation, to explore the natural history of luck across many plant and animal models. We explored the relationships among different measures of luck: variance and skewness in both lifespan and lifetime reproductive output (LRO). Furthermore, we asked: in what settings (*e.g.*, taxa, life history strategies, population growth vs. decline) does luck (of various kinds) play a large role in determining an individual's lifespan or LRO?

Our first result, that there is a positive relationship between variance in lifespan and variance in LRO, contradicts the results of another study, also using models from the COM(P)ADRE databases. Varas Enríquez et al. (2022) found no relationship between variance in LRO and standard deviation of longevity. When we calculated variance in lifespan and LRO using raw offspring counts, rather than offspring weighted by probability of survival to reproduce, we also found no correlation between these measures (not shown). However, as outlined in the Methods, we used offspring weighting to standardize the units of reproductive output. Much of the cross-species variation in LRO variance using raw offspring counts results from the difference between producing many offspring with high juvenile mortality, and producing few offspring with low juvenile mortality. Our standardization removes or at least ameliorates this source of between-species variation, making it possible to detect the expected correlation between variance in lifespan and variance in LRO.

We found that growing populations ($\lambda > 1$) had higher variances in lifespan and LRO than shrinking populations, and their variance in LRO was dominated by survival luck instead of fecundity luck. We hypothesized that the unexpected correlations between λ and variance in lifetime success might be the result of λ and lifetime success variance both having positive correlations with some third variable. We explored several candidates for what that third variable might be: stable population (st)age structure, mean lifespan, and the relative total elasticities of λ or net reproductive rate (R_0) to survival versus fecundity. However, in our collection of empirical models none of these candidates proved to have nontrivial (or any) positive correlations with both λ and lifetime success variance.

Possibly the most important results of this paper are the observed negative relationships between variance and skewness. Skewness in lifespan or LRO both tended to decrease with increasing variance in lifespan or LRO (Fig. 1A,D and Fig. S6). This confounds the often-repeated justification of the study of drivers of variance as a way to understand drivers of high reproductive skew. We found instead that populations with very high variance tend to be those with many opportunities to reproduce (precocious, highly iteroparous, and large average clutch sizes, Figure S9), and the resulting LRO has a wide distribution, but low skew. The distinct drivers of variance and skewness are further revealed by our decomposition analysis of variance and skewness. We found that variance in lifespan and LRO were determined jointly by survival, growth, and fecundity luck (Figure

3 and S16), but that skewness in both lifespan and LRO were overwhelmingly due to survival luck, with the other components decreasing skewness.

Although variance in LRO does not predict reproductive skew, it still creates inequality among individuals in their contribution to future generations, and consequently high LRO variance increases genetic drift. In particular, Hill (1972) showed that the effective population size is inversely proportional to the variance of LRO, all else being equal, even with overlapping generations. Skewness and other properties of the LRO distribution also have evolutionary impacts. For example, LRO variance alone is not sufficient to predict the fixation probability of a weakly beneficial allele (Tuljapurkar and Zuo, 2022).

Loss of genome-wide genetic variation, due to luck-based drift or other factors, can be a significant risk factor in small populations of conservation concern (Kardos et al., 2021). Plant species classified as vulnerable, endangered, or critically endangered (IUCN) are more likely to have negative population growth rates, and their life history strategies were characterised by relatively fast growth, short mature life expectancy, low iteroparity, and low reproductive output (Salguero-Gómez, 2017). Based on our results, luck is unlikely to further work against these endangered taxa. Instead, we expect the greatest variance in LRO in rapidly growing populations, and in populations with a long mature life expectancy, high clutch size, and high iteroparity. Therefore, we would expect especially high and worrisome genetic drift in populations recovering from disturbances. This has important implications for population resilience (Capdevila et al., 2022) and the preservation of intraspecific biodiversity.

On the whole, our results show that between-species variation in longevity drives most of the patterns relating luck to life history strategy. We found a positive relationship between longevity and variance in lifespan, in line with evidence that taxa with slow life histories exhibit greater variation in lifespan (Van de Walle et al., 2023). This is in contrast to work on aging in humans and primates (Colchero et al., 2016) and angiosperm plants (Baudisch et al., 2013) that found higher longevity to be associated with greater senescence and lower variance in lifespan. Many of the other life history traits we examined were positively related to longevity, so transitive logic explains many of the observed relationships between life history traits and the response variables. Clutch size is not positively related to longevity, but may be connected to longevity through a life history trade-off (Van de Walle et al., 2023). High parental investment per offspring in mammals (*i.e.* small clutch size, late age of weaning) was associated with greater early-life survivorship and a shift in the pattern of survivorship and longevity (Lynch et al., 2010). From the perspective of adults, individuals that invest heavily in reproduction tend to reach smaller terminal sizes and have shorter lifespans, so we expect a negative correlation between longevity and clutch size (Stearns, 1989), as we observed (Fig. 2): overall, large clutch size is a hallmark of a "fast" life history.

We found that the patterns among our response variables were strong and consistent across both plants and animals (Figure 1), but that plants and animals showed differing relationships between life history traits and luck (Figure 2). Plants and animals have broadly similar patterns of variance and skewness of lifetime reproductive output, but the axes of life history strategies (when variance and skewness are included) differ between plants and animals (Varas Enríquez et al., 2022). The disparity in how life history traits relate to measures of luck could be due to both real differences in life history of plants and animals (*e.g.*, retrogression and dormancy in plants) and differences in modeling approaches (*i.e.*, animals tend to be modeled with ages or developmental stages, while plants are overwhelming modeled with size classes).

Geographic, taxonomic, and life history biases in ecological research significantly limit our ability to answer ecological questions and monitor biodiversity. Species occurrence data in biodiversity databases covers only 6.74% of the globe, with observations concentrated in the Global North (Hughes et al., 2021). Taxonomically, public interest rather than research effort correlated with biodiversity coverage, with major underrepresentation of all classes of invertebrate animals, as well as fungi, lichens, ferns, mosses, and algae (Troudet et al., 2017). Similarly, observations in our dataset were concentrated in the Global North and in species of management interest for harvesting or conservation. Demographic studies in animals that met our screening criteria came primarily from vertebrates (93.5%), particularly mammals (59.5%), birds (18%), and bony fish (11.5%), whereas about 90% of named animal species are invertebrates, with insects making up about 75%. In plants, we excluded all models with clonal reproduction, despite the importance and commonness of clonal reproduction in plants. In order to census clonal plants, researchers must choose thresholds (*e.g.*, distance from the parent plant) for determining where one individual ends and another begins. These thresholds introduce variation that would confound our cross-model comparisons of luck measures. Future work should focus on standardizing demographic methods for analyzing populations that exhibit clonal reproduction and expanding the number of models available for invertebrate taxa.

In conclusion, we found that our four measures of luck — the response variables (1) variance in lifespan, (2) variance in LRO, (3) skewness of lifespan, and (4) skewness of LRO — showed remarkable range across the available demographic models for plants and animals. We found that populations with high variance in lifespan tend to have high variance in LRO as well, because an individual's lifespan controls their opportunities for reproduction in these discrete time models. We found that high variance in a given lifetime outcome does not predict high skewness, and therefore we conclude that variance by itself is not a complete measure of inequality in LRO and longevity. Longevity (mean lifespan of individuals that reproduce at least once) emerged as an important life history trait, and survival luck played a strong role in determining whether an individual achieved

particularly high reproductive output, as well as whether they lived particularly long. We found that survival luck dominates variance in LRO in growing populations, while fecundity luck is more important in shrinking populations. Taken together, our results suggest that genetic drift due to variance in LRO could prove detrimental to recovering populations of long-lived iteroparous species.

Acknowledgments

This research was supported by US NSF grants DEB-1933497 (CMH, SPE & GH) and DEB-1933612 (RES). We are very grateful to Roberto Salguero-Gomez and the COMPADRE/Padrino teams for building and maintaining databases of structured population models. We thank Peter Adler, Chris Terry, Sam Gascoigne and three anonymous reviewers for comments on the manuscript.

References

Allainé, D., D. Pontier, J. M. Gaillard, J. D. Lebreton, J. Trouvilliez, and J. Clobert. 1987. The relationship between fecundity and adult body weight in homeotherms. Oecologia **73**:478–480.

Baudisch, A., R. Salguero-Gómez, O. R. Jones, T. Wrycza, C. Mbeau-Ache, M. Franco, and F. Colchero. 2013. The pace and shape of senescence in angiosperms. Journal of Ecology **101**:596–606.

Bienvenu, F., and S. Legendre. 2015. A new approach to the generation time in matrix population models. American Naturalist **185**:834–843.

Brillinger, D. 1969. The calculation of cumulants via conditioning. Annals of the Institute of Statistical Mathematics **21**:215 – 218.

Capdevila, P., I. Stott, J. Cant, M. Beger, G. Rowlands, M. Grace, and R. Salguero-Gómez. 2022. Life history mediates the trade-offs among different components of demographic resilience. Ecology Letters .

Caswell, H. 2001. Matrix Population Models. 2 edition. Sinauer Associates, Sunderland, MA.

Caswell, H. 2013. Sensitivity analysis of discrete Markov chains via matrix calculus. Linear Algebra and its Applications **438**:1727–1745.

Cochran, M. E., and S. Ellner. 1992. Simple Methods for Calculating Age-Based Life History Parameters for Stage-Structured Populations. Ecological Monographs **62**:345–364.

Colchero, F., R. Rau, O. R. Jones, J. A. Barthold, D. A. Conde, A. Lenart, L. Nemeth, A. Scheuerlein, J. Schoeley, C. Torres, V. Zarulli, J. Altmann, D. K. Brockman, A. M. Bronikowski, L. M. Fedigan, A. E. Pusey, T. S. Stoinski, K. B. Strier, A. Baudisch, S. C. Alberts, and J. W. Vaupel. 2016. The emergence of longevous populations. Proceedings of the National Academy of Sciences **113**.

De Roos, A. M., L. Persson, and E. McCauley. 2003. The influence of size-dependent life-history traits on the structure and dynamics of populations and communities. Ecology Letters **6**:473–487.

Demetrius, L. 1977. Measures of fitness and demographic stability. Proceedings of the National Academy of Sciences **74**:384–386.

Demetrius, L., S. Legendre, and P. Harremöes. 2009. Evolutionary Entropy: A Predictor of Body Size, Metabolic Rate and Maximal Life Span. Bulletin of Mathematical Biology **71**.

Dietze, M. C. 2017. Prediction in ecology: a first-principles framework. Ecological Applications **27**:2048–2060.

Ellner, S. P. 2018. Generation time in structured populations. American Naturalist **192**:105–110.

Ellner, S. P., D. Z. Childs, and M. Rees. 2016. Data-driven Modelling of Structured Populations: A Practical Guide to the Integral Projection Model. Springer International Publishing, Cham.

Eusemann, P., and H. Liesebach. 2021. Small-scale genetic structure and mating patterns in an extensive sessile oak forest (*Quercus petraea* (Matt.) Liebl.). Ecology and Evolution **11**:7796–7809.

Gerzabek, G., S. Oddou-Muratorio, and A. Hampe. 2017. Temporal change and determinants of maternal reproductive success in an expanding oak forest stand. Journal of Ecology **105**:39–48.

Goodwin, J. C. A., R. A. King, J. I. Jones, A. Ibbotson, and J. R. Stevens. 2016. A small number of anadromous females drive reproduction in a brown trout (*Salmo trutta*) population in an English chalk stream. Freshwater Biology **61**:1075–1089.

Healy, K., T. H. G. Ezard, O. R. Jones, R. Salguero-Gómez, and Y. M. Buckley. 2019. Animal life history is shaped by the pace of life and the distribution of age-specific mortality and reproduction. Nature Ecology & Evolution **3**:1217–1224.

Hernández, C. M., S. P. Ellner, R. E. Snyder, and G. Hooker. 2023. Supplemental code and data for Hernández et al. "The natural history of luck: A synthesis study of structured population models". Zenodo URL `doi.org/10.5281/zenodo.8199887`.

Hernández, C. M., S. P. Ellner, P. B. Adler, G. Hooker, and R. E. Snyder. 2023. An exact version of Life Table Response Experiment analysis, and the R package exactLTRE. Methods in Ecology and Evolution **14**:939–951.

Hill, W. G. 1972. Effective Size of Populations with Overlapping Generations. Theoretical Population Biology **3**:278–289.

Hixon, M. a., D. W. Johnson, and S. M. Sogard. 2014. BOFFFFs: on the importance of conserving old-growth age structure in fishery populations. ICES Journal of Marine Science **71**:2171–2185.

Houde, E. D. 1989. Comparative growth, mortality, and energetics of marine fish larvae: temperature and implied latitudinal effects. Fishery Bulletin **87**:471–495.

Hughes, A. C., M. C. Orr, K. Ma, M. J. Costello, J. Waller, P. Provoost, Q. Yang, C. Zhu, and H. Qiao. 2021. Sampling biases shape our view of the natural world. Ecography **44**:1259–1269.

Jenouvrier, S., L. Aubry, S. van Daalen, C. Barbraud, H. Weimerskirch, and H. Caswell. 2022. When the going gets tough, the tough get going: Effect of extreme climate on an Antarctic seabird's life history. Ecology Letters .

Jones, O. R., P. Barks, I. Stott, T. D. James, S. Levin, W. K. Petry, P. Capdevila, J. Che-Castaldo, J. Jackson, G. Römer, C. Schuette, C. C. Thomas, and R. Salguero-Gómez. 2022. Rcompadre and Rage—Two R packages to facilitate the use of the COMPADRE and COMADRE databases and calculation of life-history traits from matrix population models. Methods in Ecology and Evolution **13**:770–781.

Juanes, F., and D. O. Conover. 1994. Piscivory and prey size selection in young-of-the-year bluefish: predator preference or size-dependent capture success? Marine Ecology Progress Series pages 59–69.

Kardos, M., E. E. Armstrong, S. W. Fitzpatrick, S. Hauser, P. W. Hedrick, J. M. Miller, D. A. Tallmon, and W. C. Funk. 2021. The crucial role of genome-wide genetic variation in conservation. Proceedings of the National Academy of Sciences **118**.

Kendall, B. E., M. Fujiwara, J. Diaz-Lopez, S. Schneider, J. Voigt, and S. Wiesner. 2019. Persistent problems in the construction of matrix population models. Ecological Modelling **406**:33–43.

Le Boeuf, B., R. Condit, and J. Reiter. 2019. Lifetime reproductive success of northern elephant seals (*Mirounga angustirostris*). Canadian Journal of Zoology **97**:1203–1217.

Levin, S. C., S. Evers, T. Potter, M. P. Guerrero, D. Z. Childs, A. Compagnoni, T. M. Knight, and R. Salguero-Gómez. 2022. Rpadrino: An R package to access and use PADRINO, an open access database of Integral Projection Models. Methods in Ecology and Evolution **13**:1923–1929.

Lynch, H. J., S. Zeigler, L. Wells, J. D. Ballou, and W. F. Fagan. 2010. Survivorship patterns in captive mammalian populations: Implications for estimating population growth rates. Ecological Applications **20**:2334–2345.

Maino, J. L., M. R. Kearney, R. M. Nisbet, and S. A. L. M. Kooijman. 2014. Reconciling theories for metabolic scaling. Journal of Animal Ecology **83**:20–29.

Munguía-Rosas, M. A., J. Ollerton, V. Parra-Tabla, and J. A. De-Nova. 2011. Meta-analysis of phenotypic selection on flowering phenology suggests that early flowering plants are favoured. Ecology Letters **14**:511–521.

Pauly, D. 1980. On the interrelationships between natural mortality, growth parameters, and mean environmental temperature in 175 fish stocks. ICES Journal of Marine Science **39**:175–192.

Ross, C. T., P. L. Hooper, J. E. Smith, A. V. Jaeggi, E. A. Smith, S. Gavrilets, F. tuz Zohora, J. Ziker, D. Xygalatas, E. E. Wroblewski, B. Wood, B. Winterhalder, K. P. Willführ, A. K. Willard, K. Walker, C. von Rueden, E. Voland, C. Valeggia, B. Vaitla, S. Urlacher, M. Towner, C.-Y. Sum, L. S. Sugiyama, K. B. Strier, K. Starkweather, D. Major-Smith, M. Shenk, R. Sear, E. Seabright, R. Schacht, B. Scelza, S. Scaggs, J. Salerno, C. Revilla-Minaya, D. Redhead, A. Pusey, B. G. Purzycki, E. A. Power, A. Pisor, J. Pettay, S. Perry, A. E. Page, L. Pacheco-Cobos, K. Oths, S.-Y. Oh, D. Nolin, D. Nettle, C. Moya, A. B. Migliano, K. J. Mertens, R. A. McNamara, R. McElreath, S. Mattison, E. Massengill, F. Marlowe, F. Madimenos, S. Macfarlan, V. Lummaa, R. Lizarralde, R. Liu, M. A. Liebert, S. Lew-Levy, P. Leslie, J. Lanning, K. Kramer, J. Koster, H. S. Kaplan, B. Jamsranjav, A. M. Hurtado, K. Hill, B. Hewlett, S. Helle, T. Headland, J. Headland, M. Gurven, G. Grimalda, R. Greaves, C. D. Golden, I. Godoy, M. Gibson, C. E. Mouden, M. Dyble, P. Draper, S. Downey, A. L. DeMarco, H. E. Davis, S. Crabtree, C. Cortez, H. Colleran, E. Cohen, G. Clark, J. Clark, M. A. Caudell, C. E. Carminito, J. Bunce, A. Boyette, S. Bowles, T. Blumenfield, B. Beheim, S. Beckerman, Q. Atkinson, C. Apicella, N. Alam, and M. B. Mulder. 2023. Reproductive inequality in humans and other mammals. Proceedings of the National Academy of Sciences **120**.

Salguero-Gómez, R., O. R. Jones, C. R. Archer, C. Bein, H. de Buhr, C. Farack, F. Gottschalk, A. Hartmann, A. Henning, G. Hoppe, G. Römer, T. Ruoff, V. Sommer, J. Wille, J. Voigt, S. Zeh, D. Vieregg, Y. M. Buckley, J. Che-Castaldo, D. Hodgson, A. Scheuerlein, H. Caswell, and J. W.

Vaupel. 2016. COMADRE: A global data base of animal demography. Journal of Animal Ecology **85**:371–384.

Salguero-Gómez, R., O. R. Jones, E. Jongejans, S. P. Blomberg, D. J. Hodgson, C. Mbeau-Ache, P. A. Zuidema, H. D. Kroon, and Y. M. Buckley. 2016. Fast-slow continuum and reproductive strategies structure plant life-history variation worldwide. Proceedings of the National Academy of Sciences of the United States of America **113**:230–235.

Salguero-Gómez, R. 2017. Applications of the fast–slow continuum and reproductive strategy framework of plant life histories. New Phytologist **213**:1618–1624.

Salguero-Gómez, R., O. R. Jones, C. R. Archer, Y. M. Buckley, J. Che-Castaldo, H. Caswell, D. Hodgson, A. Scheuerlein, D. A. Conde, E. Brinks, H. Buhr, C. Farack, F. Gottschalk, A. Hartmann, A. Henning, G. Hoppe, G. Römer, J. Runge, T. Ruoff, J. Wille, S. Zeh, R. Davison, D. Vieregg, A. Baudisch, R. Altwegg, F. Colchero, M. Dong, H. Kroon, J. Lebreton, C. J. E. Metcalf, M. M. Neel, I. M. Parker, T. Takada, T. Valverde, L. A. Vélez-Espino, G. M. Wardle, M. Franco, and J. W. Vaupel. 2015. The COMPADRE Plant Matrix Database: an open online repository for plant demography. Journal of Ecology **103**:202–218.

Snyder, R. E., and S. P. Ellner. 2016. We Happy Few: Using Structured Population Models to Identify the Decisive Events in the Lives of Exceptional Individuals. The American Naturalist **188**:E28–E45.

Snyder, R. E., and S. P. Ellner. 2018. Pluck or luck: Does trait variation or chance drive variation in lifetime reproductive success? American Naturalist **191**:E90–E107.

Snyder, R. E., and S. P. Ellner. 2022. Snared in an Evil Time: How Age-Dependent Environmental and Demographic Variability Contribute to Variance in Lifetime Outcomes. American Naturalist **200**:E124–E140.

Snyder, R. E., and S. P. Ellner. 2023. To prosper, live long: understanding the sources of reproductive skew and extreme reproductive success in structured populations. *in prep.* .

Snyder, R. E., S. P. Ellner, and G. Hooker. 2021. Time and Chance: Using Age Partitioning to Understand How Luck Drives Variation in Reproductive Success. The American Naturalist **197**:E110–E128.

Stearns, S. C. 1989. Trade-Offs in Life-History Evolution. Functional Ecology **3**:259–268.

Troudet, J., P. Grandcolas, A. Blin, R. Vignes-Lebbe, and F. Legendre. 2017. Taxonomic bias in biodiversity data and societal preferences. Scientific Reports **7**:9132.

738 Tuljapurkar, S., and W. Zuo. 2022. Mutations and the Distribution of Lifetime Reproductive
739 Success. Journal of the Indian Institute of Science **102**:1269 – 1275.

740 Tuljapurkar, S., W. Zuo, T. Coulson, C. Horvitz, and J. M. Gaillard. 2020. Skewed distributions
741 of lifetime reproductive success: beyond mean and variance. Ecology Letters **23**:748–756.

742 van Daalen, S. F., and H. Caswell. 2017. Lifetime reproductive output: individual stochasticity,
743 variance, and sensitivity analysis. Theoretical Ecology **10**:355–374.

744 van Daalen, S. F., C. M. Hernández, H. Caswell, M. G. Neubert, and K. E. Gribble. 2022. The
745 Contributions of Maternal Age Heterogeneity to Variance in Lifetime Reproductive Output. The
746 American Naturalist **199**:603–616.

747 Van de Walle, J., R. Fay, J.-M. Gaillard, F. Pelletier, S. Hamel, M. Gamelon, C. Barbraud, F. G.
748 Blanchet, D. T. Blumstein, A. Charmantier, K. Delord, B. Larue, J. Martin, J. A. Mills, E. Milot,
749 F. M. Mayer, J. Rotella, B.-E. Saether, C. Teplitsky, M. van de Pol, D. H. Van Vuren, M. E.
750 Visser, C. P. Wells, J. Yarrall, and S. Jenouvrier. 2023. Individual life histories: neither slow nor
751 fast, just diverse. Proceedings of the Royal Society B: Biological Sciences **290**:20230511.

752 Van Valen, L. 1975. Life, Death, and Energy of a Tree. Biotropica **7**:259.

753 Varas Enríquez, P. J., S. van Daalen, and H. Caswell. 2022. Individual stochasticity in the life
754 history strategies of animals and plants. PLOS ONE **17**:e0273407.

755 Weiner, J., L. G. Campbell, J. Pino, and L. Echarte. 2009. The allometry of reproduction within
756 plant populations. Journal of Ecology **97**:1220–1233.

757 West, G. B., J. H. Brown, and B. J. Enquist. 1997. A General Model for the Origin of Allometric
758 Scaling Laws in Biology. Science **276**:122–126.

Section S1 Mean, variance, and skewness of lifetime reproductive output

For calculating mean, variance, and skewness in lifetime reproductive output (LRO), we used the framework of Markov Chains with rewards following van Daalen and Caswell (2017). We assumed that annual offspring production has a Poisson distribution, so we reproduce the equations for that case here.

In this framework, the life cycle is represented by a Markov Chain with death as the unique absorbing state, and all living states are transient. The population projection matrix ($\mathbf{A} = \mathbf{U} + \mathbf{F}$) describes only the τ transient states. With death included as the absorbing state, the state transition matrix is

$$\mathbf{P} = \left(\begin{array}{c|c} \mathbf{U}_{\tau\times\tau} & \mathbf{0}_{\tau\times 1} \\ \hline \mathbf{M}_{1\times\tau} & 1 \end{array} \right), \tag{S1}$$

where $\mathbf{M}$ is a row of mortality probabilities, generated by taking the difference between 1 and the column sums of $\mathbf{U}$. We also need to define $\mathbf{Z}$, an operator matrix that cleaves off the absorbing state:

$$\mathbf{Z} = \left(\begin{array}{c|c} \mathbf{I}_{\tau\times\tau} & \mathbf{0}_{\tau\times 1} \end{array} \right), \tag{S2}$$

and the $\tau \times \tau$ submatrix of reward/moment corresponding to transitions among the transient states:

$$\widetilde{\mathbf{R}}_k = \mathbf{Z}\mathbf{R}_k\mathbf{Z}^{\mathsf{T}} \tag{S3}$$

The matrix $\mathbf{R}_1$ giving the first moment of the rewards for each state transition, is given by:

$$\mathbf{R}_1 = \mathbf{1}_{\tau+1}(\mathbf{f}^{\mathsf{T}}|\mathbf{0}_{1\times 1}), \tag{S4}$$

where $\mathbf{f}$ is the stage-specific total fertility rewards. Prior to this calculatin we re-scaled $\mathbf{F}$, weighting offspring by their probability of surviving to reproduce (this is described fully in the main text, section 4.3); then $\mathbf{f}$ is given by the column sums of the re-scaled fertility matrix.

For Poisson-distributed annual rewards, the matrices giving the second and third moments of reward are:

$$\mathbf{R}_2 = \mathbf{R}_1 + (\mathbf{R}_1 \circ \mathbf{R}_1) \tag{S5}$$

$$\mathbf{R}_3 = \mathbf{R}_1 + 3(\mathbf{R}_1 \circ \mathbf{R}_1) + (\mathbf{R}_1 \circ \mathbf{R}_1 \circ \mathbf{R}_1) \tag{S6}$$

where $\circ$ denotes the Hadamard (element-by-element) product of equal-size matrices or vectors.

Notation We now need to introduce notation for moments of a distribution. We use $\mu_k(X)$ for the k-th central moment of the random variable X, and $\mu'_k(X)$ for the k-th raw (*i.e.*, non-central) moment of X. We use $\widetilde{\mu}_3$ to denote skewness. We use bold symbols ($\boldsymbol{\mu}$) to indicate the vector of the given moment conditional on possible starting states. We use ρ to denote LRO considered as a random variable. In this section, all equations for moments refer to moments of ρ, but we use the notation just described for moments in general.

The moments of lifetime accumulated reproductive output, conditional on starting state z_0, are:

$$\boldsymbol{\mu}'_1 = \mathbf{N}^{\mathsf{T}}\mathbf{Z}(\mathbf{P}\circ\mathbf{R}_1)^{\mathsf{T}}\mathbf{1}_{\tau+1} \tag{S7}$$

$$\boldsymbol{\mu}'_2 = \mathbf{N}^{\mathsf{T}}\left[\mathbf{Z}(\mathbf{P}\circ\mathbf{R}_2)^{\mathsf{T}}\mathbf{1}_{\tau+1} + 2\left(\mathbf{U}\circ\widetilde{\mathbf{R}}_1\right)^{\mathsf{T}}\boldsymbol{\mu}'_1\right] \tag{S8}$$

$$\boldsymbol{\mu}'_3 = \mathbf{N}^{\mathsf{T}}\left[\mathbf{Z}(\mathbf{P}\circ\mathbf{R}_3)^{\mathsf{T}}\mathbf{1}_{\tau+1} + 3\left(\mathbf{U}\circ\widetilde{\mathbf{R}}_2\right)^{\mathsf{T}}\boldsymbol{\mu}'_1 + 3\left(\mathbf{U}\circ\widetilde{\mathbf{R}}_1\right)^{\mathsf{T}}\boldsymbol{\mu}'_2\right]. \tag{S9}$$

These can be used to generate the central moments, as vectors conditional on starting state (NB: variance is the second central moment):

$$\boldsymbol{\mu}_2 = \boldsymbol{\mu}'_2 - \boldsymbol{\mu}'_1\circ\boldsymbol{\mu}'_1 \tag{S10}$$

$$\boldsymbol{\mu}_3 = \boldsymbol{\mu}'_3 - 3(\boldsymbol{\mu}'_2\circ\boldsymbol{\mu}'_1) + 2(\boldsymbol{\mu}'_1\circ\boldsymbol{\mu}'_1\circ\boldsymbol{\mu}'_1) \tag{S11}$$

Section S1.1 Variance in LRO

The variance in LRO, conditional on the starting state, is the second central moment (Eqn. S10). The variance in LRO, taken across the mixing distribution, is given by:

$$\begin{aligned} Var(\rho) &= \mathbb{E}\left(Var(\rho|z_0)\right) + Var\left(\mathbb{E}(\rho|z_0)\right) \\ &= \boldsymbol{\mu}_2^{\mathsf{T}}\boldsymbol{\pi}_z + \left((\boldsymbol{\mu}'_1)^2\right)^{\mathsf{T}}\boldsymbol{\pi}_z - \left(\boldsymbol{\mu}'_1\boldsymbol{\pi}_z\right)^2 \end{aligned} \tag{S12}$$

Section S1.2 Skewness of LRO

Skewness, conditional on starting state, is given by:

$$\widetilde{\boldsymbol{\mu}}_3 = \boldsymbol{\mu}_3\circ\boldsymbol{\mu}_2^{(-3/2)} \tag{S13}$$

In order to calculate the total skewness, for a cohort described by a mixing distribution over initial state, we first need to calculate the total third central moment. Because the third cumulant of a random variable equals its third central moment, we can use the law of total cumulance (Brillinger,

1969) for the third cumulant:

$$\mu_3(\rho) = \mathbb{E}(\mu_3(\rho|z_0)) + \mu_3\left(\mathbb{E}(\rho|z_0)\right) + 3\, Cov\left(\mathbb{E}(\rho|z_0),\, Var(\rho|z_0)\right). \tag{S14}$$

where the expectations and covariance are all with respect to the distribution of z_0.

The first term, the expected value of the third central moment of LRO, is:

$$\mathbb{E}(\mu_3(\rho|z_0)) = \boldsymbol{\mu}_3^{\mathsf{T}}\boldsymbol{\pi}_z. \tag{S15}$$

The second term is the third central moment (with respect to $\boldsymbol{\pi}_z$) of $\mathbb{E}(\rho|z_0)$ For any random variable X, $\mu_3(X) = \mathbb{E}\left[(X-\bar{X})^3\right]$, and $\mathbb{E}\left[\mathbb{E}(X|z_0)\right] = \mathbb{E}(X)$. Therefore

$$\begin{aligned}\mu_3\left(\mathbb{E}(\rho|z_0)\right) &= \mathbb{E}\left[\left(\mathbb{E}(\rho|z_0) - \mathbb{E}(\rho)\right)^3\right] \\ &= \left[\left(\boldsymbol{\mu}_1' - \left((\boldsymbol{\mu}_1')^{\mathsf{T}}\boldsymbol{\pi}_z\right)\right)^3\right]^{\mathsf{T}}\boldsymbol{\pi}_z \end{aligned} \tag{S16}$$

The third term, the covariance of the expected value and the variance of LRO, is given by:

$$\begin{aligned} Cov\Big(\mathbb{E}(X|Y),\, Var(X|Y)\Big) &= \mathbb{E}\Big(\mathbb{E}(X|Y)\times Var(X|Y)\Big) - \mathbb{E}\Big(\mathbb{E}(X|Y)\Big)\times\mathbb{E}\Big(Var(X|Y)\Big) \\ &= (\boldsymbol{\mu}_1'\circ\boldsymbol{\mu}_2)^{\mathsf{T}}\boldsymbol{\pi}_z - \Big((\boldsymbol{\mu}_1')^{\mathsf{T}}\boldsymbol{\pi}_z\Big)\left(\boldsymbol{\mu}_2^{\mathsf{T}}\boldsymbol{\pi}_z\right) \end{aligned} \tag{S17}$$

Section S2 Mean, variance, and skewness of lifespan

The mean, variance, and skewness of lifespan can be calculated using a Markov Chain with rewards, where individuals receive exactly 1 reward for each time step they survive. This can be achieved following the "fixed rewards" case of van Daalen and Caswell (2017, Eqn. 8 and 9). However, the equations for mean, variance, and skewness in lifespan can also be written in simpler equation forms. In what follows, we present these simpler equations, following Caswell (2013) and Ellner et al. (2016).

Section S2.1 Mean Lifespan

The vector of expected future lifespan given current state z_0 of an individual is

$$\mathbb{E}(L|z_0) = \mathbf{e}^{\mathsf{T}}\mathbf{N}, \tag{S18}$$

where $\mathbf{e}^{\mathsf{T}}$ is a column vector of 1's with the same length as the number of classes in $\mathbf{A}$. The fundamental matrix $\mathbf{N}$ contains the expected number of time steps that an individual will spend

in each age, stage, or size class during their lifespan, given their current state. $\mathbf{N}$ is calculated as:

$$\mathbf{N} = (\mathbf{I} - \mathbf{U})^{-1}, \tag{S19}$$

where $\mathbf{U}$ is the matrix containing all of the non-reproductive transitions of $\mathbf{A}$ (*i.e.*, survival, growth, and retrogression) and $\mathbf{I}$ is an identity matrix with the same dimensions as $\mathbf{U}$.

The overall expected lifespan, for a cohort having a mixing distribution $\boldsymbol{\pi}_z$ for possible initial states z_i, is

$$\mathbb{E}(L) = \sum_i (\mathbb{E}(L|z_0 = z_i)\mathbb{P}(z_0 = z_i)) = \mathbb{E}(L|z_0)^{\mathsf{T}}\boldsymbol{\pi}_z = \mathbf{e}^{\mathsf{T}}\mathbf{N}\boldsymbol{\pi}_z \tag{S20}$$

Section S2.2 Variance in Lifespan

The variance in lifespan, given the starting state of an individual is calculated as:

$$Var(L|z_0) = \mathbf{e}^{\mathsf{T}}\left(2\mathbf{N}^2 - \mathbf{N}\right) - \mathbf{e}^{\mathsf{T}}\mathbf{N} \circ \mathbf{e}^{\mathsf{T}}\mathbf{N} \tag{S21}$$

The total variance, for a cohort described by the mixing distribution, is given by the law of total variance:

$$Var(L) = \mathbb{E}(\,Var(L|z_0)) + \,Var(\mathbb{E}(L|z_0)). \tag{S22}$$

The first term, the variance due to uncertainty in the life-course for individuals in the same starting state, is calculated as:

$$\mathbb{E}(\,Var(L|z_0)) = \sum_i \,Var(L|z_0 = z_i)\mathbb{P}(z_0 = z_i) \tag{S23}$$

$$= \,Var(L|z_0)^{\mathsf{T}}\boldsymbol{\pi}_z \tag{S24}$$

The second term, the variance due to uncertainty in the starting state of individuals, is calculated as:

$$Var(\mathbb{E}(L|z_0)) = \mathbb{E}(\mathbb{E}(L|z_0)^2) - [\mathbb{E}(L|z_0)]^2 \tag{S25}$$

$$= \sum_i \left(\mathbb{E}(L|z_0 = z_i)\right)^2 \mathbb{P}(z_0 = z_i) - \left(\sum_i (\mathbb{E}(L|z_0 = z_i)\mathbb{P}(z_0 = z_i))\right)^2 \tag{S26}$$

$$= \left[\left(\mathbb{E}(L|z_0)\right)^2\right]^{\mathsf{T}}\boldsymbol{\pi}_z - \left(\mathbb{E}(L|z_0)^{\mathsf{T}}\boldsymbol{\pi}_z\right)^2 \tag{S27}$$

Section S2.3 Skewness in Lifespan

Equations for the first 3 raw moments of longevity conditional on starting state were presented in Caswell (2013):

$$\mu_1'(L|z_0) = (\boldsymbol{\mu}_1')^{\mathsf{T}} = \mathbf{e}^{\mathsf{T}}\mathbf{N} \tag{S28}$$

$$\mu_2'(L|z_0) = (\boldsymbol{\mu}_2')^{\mathsf{T}} = \mathbf{e}^{\mathsf{T}}\mathbf{N}(2\mathbf{N} - \mathbf{I}) \tag{S29}$$

$$\mu_3'(L|z_0) = (\boldsymbol{\mu}_3')^{\mathsf{T}} = \mathbf{e}^{\mathsf{T}}\mathbf{N}(6\mathbf{N}^2 - 6\mathbf{N} + \mathbf{I}) \tag{S30}$$

The second and third central moments are as in Equations S10–S11, and skewness is given by Equation S13.

Section S3 Longevity, the expected lifespan of individuals who reproduce at least once

As explained in the main text, longevity was calculated as the mean time to absorbtion for a modified Markov chain, eqn. (4), conditional on absorbtion into Ω_2, individuals who reproduced before they died.

The first step is to calculate the transition probabilities conditional on absorbtion. This is a standard Markov Chain technique (Caswell, 2001, ch. 5); our notation follows Snyder and Ellner (2016).

The expected number of time steps spent in each transient state, given the starting state, is the fundamental matrix ($\mathbf{N} = (\mathbf{I} - \mathbf{Q})^{-1}$) of the transient state transition matrix:

$$\mathbf{Q} = \left(\begin{array}{c|c} \mathbf{T}_{\tau\times\tau} & \mathbf{0}_{\tau\times\tau} \\ \hline \mathbf{R}_{\tau\times\tau} & \mathbf{U}_{\tau\times\tau} \end{array}\right). \tag{S31}$$

The probability of being absorbed into Ω_2, individuals who reproduced before they died, is

$$q_{\mathbb{L}} = a_{\mathbb{L}} * (\mathbf{I} - \mathbf{Q})^{-1}, \tag{S32}$$

where $a_{\mathbb{L}}$ is the one-step-ahead probability of being absorbed into Ω_2, given by ($\mathbf{0}_{1\times\tau}, \mathbf{M}_{1\times\tau}$ — zero for individuals in the first half of the extended state space (those who have not yet reproduced), and the probability of death for those in the second half.

We then calculated the transition probabilities for the transient states of $\mathbf{P}$ conditional on absorption into Ω_2 as:

$$Q_{\Omega 2}(z', z) = Q(z', z)\frac{q_{\mathbb{L}}(z')}{q_{\mathbb{L}}(z)}. \tag{S33}$$

The expected lifespan of individuals who reproduced, conditional on starting state is then:

$$\mathbb{E}(L_{\Omega 2}|z_0) = \mathbf{e}^{\mathsf{T}}(\mathbf{I} - \mathbf{Q_{\Omega 2}})^{-1}. \tag{S34}$$

The mixing distribution must be changed here to reflect the different probabilities of absorption into Ω_2 for the different starting states (Note that no individuals can start in the part of the extended state space that is individuals who have already reproduced once):

$$\pi_\Omega(z) = \frac{\pi(z)q_{\mathbb{L}}(z)}{\langle \pi_z, q_{\mathbb{L}}(z)\rangle}, \tag{S35}$$

and then the expected lifespan of individuals who reproduced, taken over the mixing distribution is:

$$\mathbb{E}(L_{\Omega 2}) = \mathbb{E}(L_{\Omega 2}|z_0)^{\mathsf{T}}\boldsymbol{\pi}_\Omega. \tag{S36}$$

Section S4 Offspring scaling and the importance of fecundity luck

A simple example illustrates how scaling offspring by their probability of surviving to reproduce will tend to increase the proportion of total luck (*i.e.*, total variance in LRO) that is due to fecundity luck. This effect of scaling explains why this paper finds many examples where fecundity luck is a substantial component of LRO variance, while previous work (Snyder et al., 2021) found that fecundity luck is relatively unimportant in general.

The example is as follows: suppose that individuals live $N \geq 1$ years where N is random and varies independently across individuals, and at age a they have B_a offspring where B_a is Poisson with mean f. In terms of our luck partition, this is a model with survival luck and fecundity luck, but no growth trajectory luck because all individuals are always the same size and have the same fecundity in each year of life.

By definition, fecundity luck is

$$\mathbb{E}_N\left[\sum_{a=1}^{N} Var(B_a)\right] = \mathbb{E}_N\left[\sum_{a=1}^{N} f\right] = \mathbb{E}(N)f. \tag{S37}$$

But the law of total variance, the variance of LRO R is

$$Var(R) = \mathbb{E}_N\, Var(R|N) + Var_N\, \mathbb{E}(R|N) = \mathbb{E}_N\, Nf + Var_N(fN) = f\,\mathbb{E}(N) + f^2\, Var(N). \tag{S38}$$

The proportion of LRO variance due to fecundity luck is therefore

$$p_{fec} = \frac{\mathbb{E}(N)}{\mathbb{E}(N) + f\ Var(N)}. \tag{S39}$$

Going from raw offspring counts, to offspring multiplied by their probability of survival to reproduce, decreases the value of f and therefore increases p_{fec}. In the limit of $f \to 0$, $p_{fec} \to 1$. However, that limit cannot ever be reached because it would give $\lambda = 0$.

If we drop the assumption that B is Poisson and therefore has equal mean and variance, we get the more general expression

$$p_{fec} = \frac{\mathbb{E}(N)\ Var(B)}{\mathbb{E}(N)\ Var(B) + Var(N)\,\mathbb{E}(B)^2}. \tag{S40}$$

The numerator is fecundity luck: what the variance in LRO would be, if everyone had exactly the expected lifespan. The denominator is fecundity luck again, plus survival luck: what the variance in LRO would be, if everyone had exactly the expected fecundity in every year that they lived.

A biological interpretation of this result is that when offspring are scaled by their probability of surviving to reproduce, the luck of surviving to reproduce or not is moved from survivalluck to fecundity luck. That is, whether an offspring survives to reproduce or dies first (in a model without offspring scaaling) is represented as a change in the number of offspring in a model with offspring scaling.

Section S5 Supplemental Figures and Tables

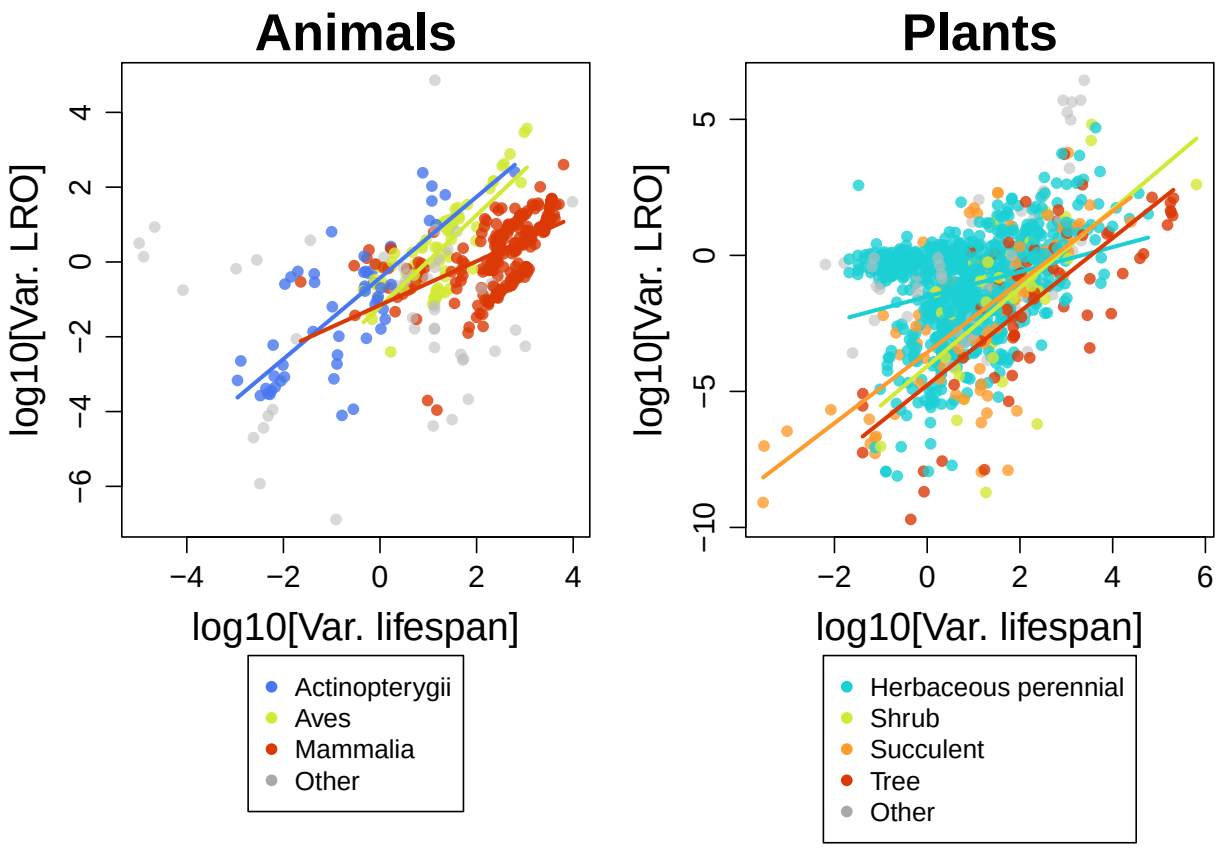

Figure S1: Relationships between luck in lifespan and luck in lifetime reproductive output for different animal taxa (at the "Class" level) and different plant growth forms. All data are plotted, but the three most common animal classes and the four most common plant growth forms are highlighted in color. For these groups, we also show the linear model for the log-transformed data. Note that the axes are log-scaled.

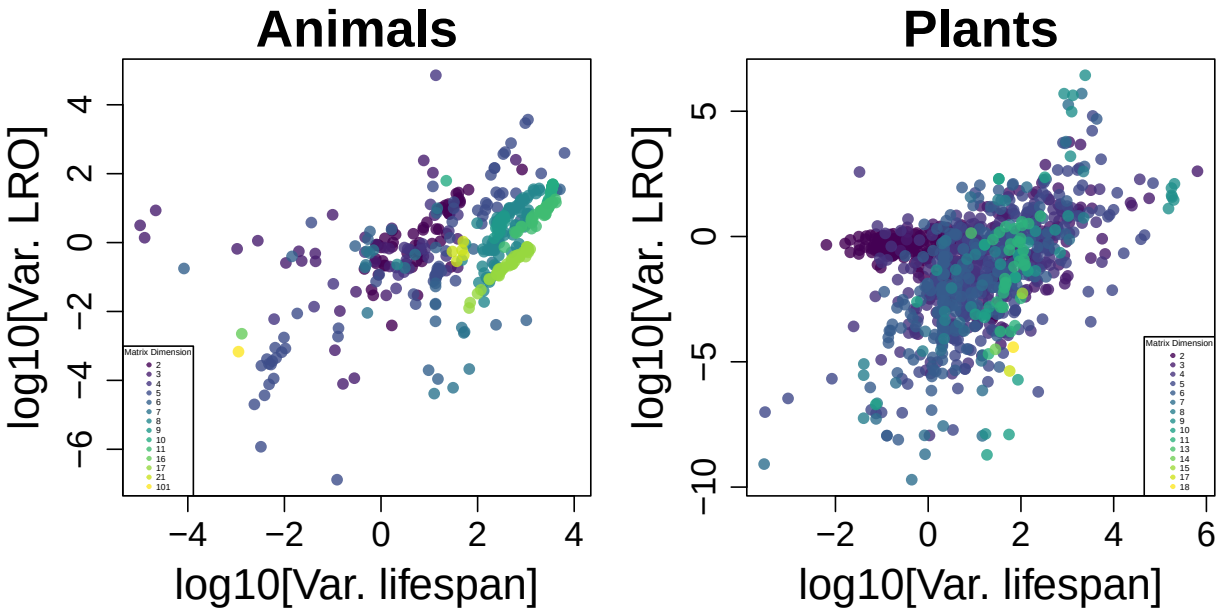

Figure S2: Relationships between luck in lifespan and luck in lifetime reproductive output, with points colored by matrix dimension (the number of i-states/stages used to classify individuals). This figure excludes integral projection models. Note that the axes are log-scaled.

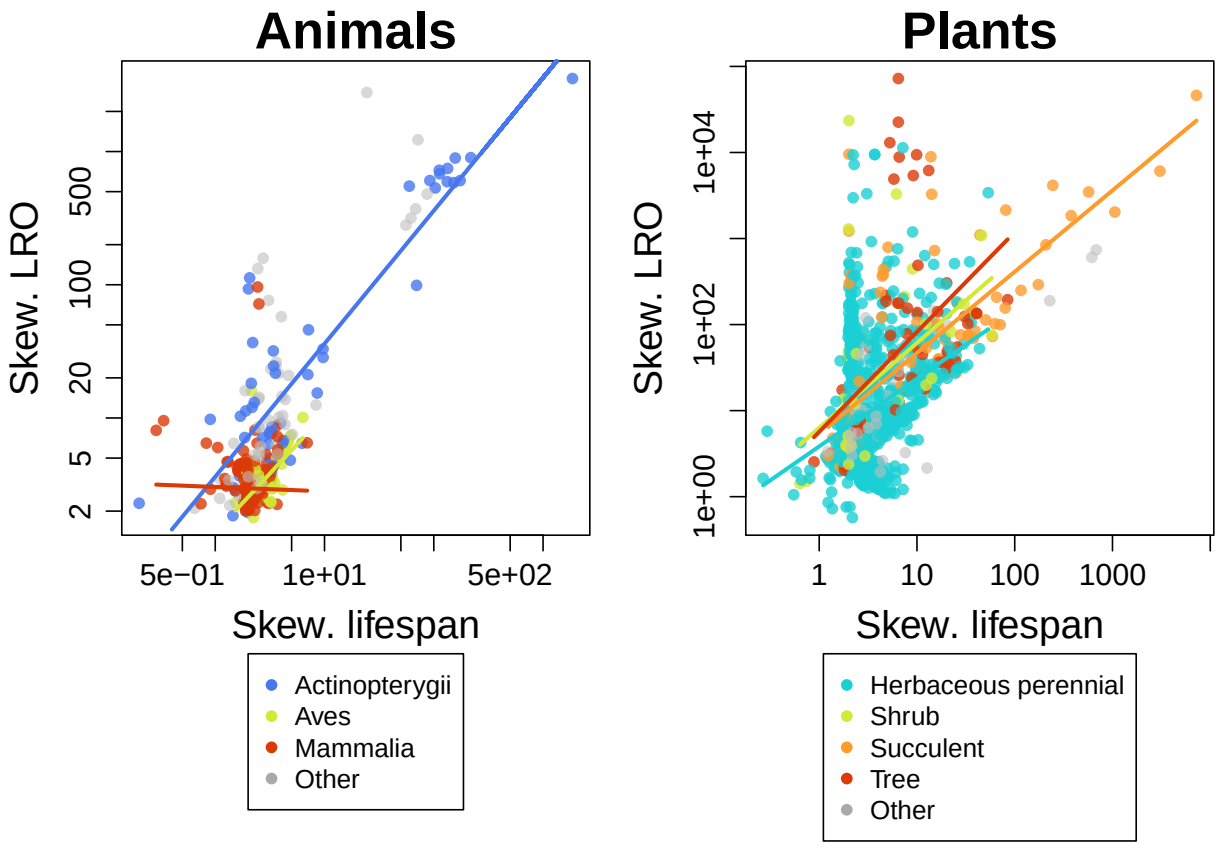

Figure S3: Relationships between skewness of lifespan and skewness of lifetime reproductive output for different animal taxa (at the "Class" level) and different plant growth forms. All data are plotted, but the three most common animal classes and the four most common plant growth forms are highlighted. For these groups, we also show the linear model for the log-transformed data. Note that the axes are log-scaled.

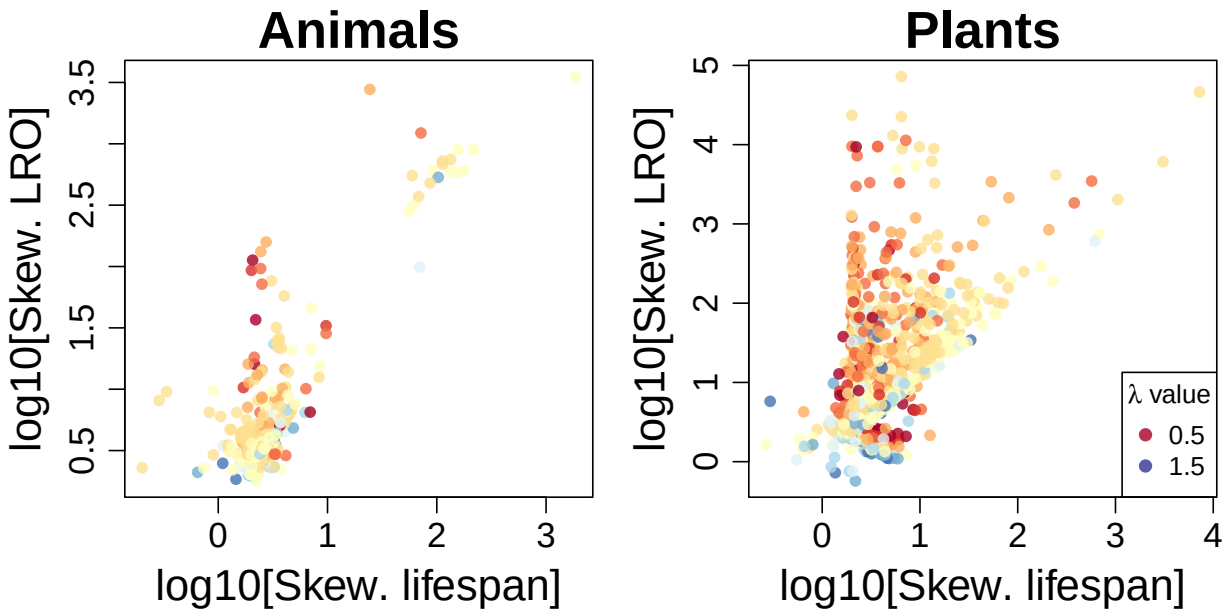

Figure S4: Relationships between skewness of lifespan and skewness of lifetime reproductive output, with points colored by population growth rate (λ, the leading eigenvalue of the projection matrix or kernel). Note that the axes are log-scaled.

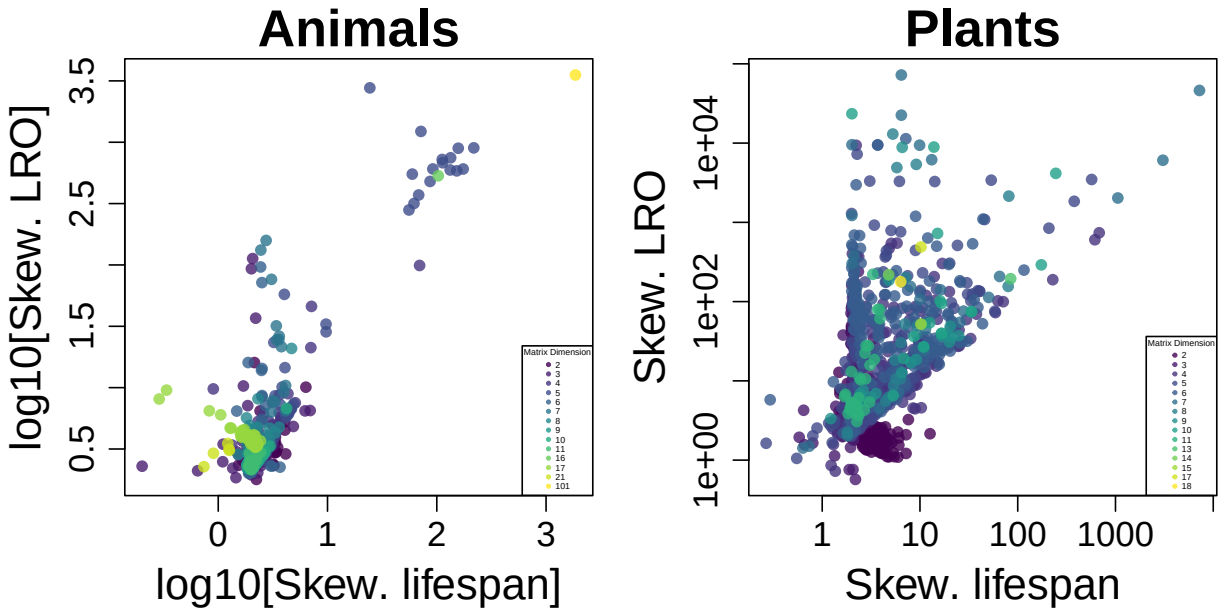

Figure S5: Relationships between skewness of lifespan and skewness of lifetime reproductive output, with points colored by matrix dimension (the number of i-states/stages used to classify individuals). This figure excludes integral projection models. Note that the axes are log-scaled.

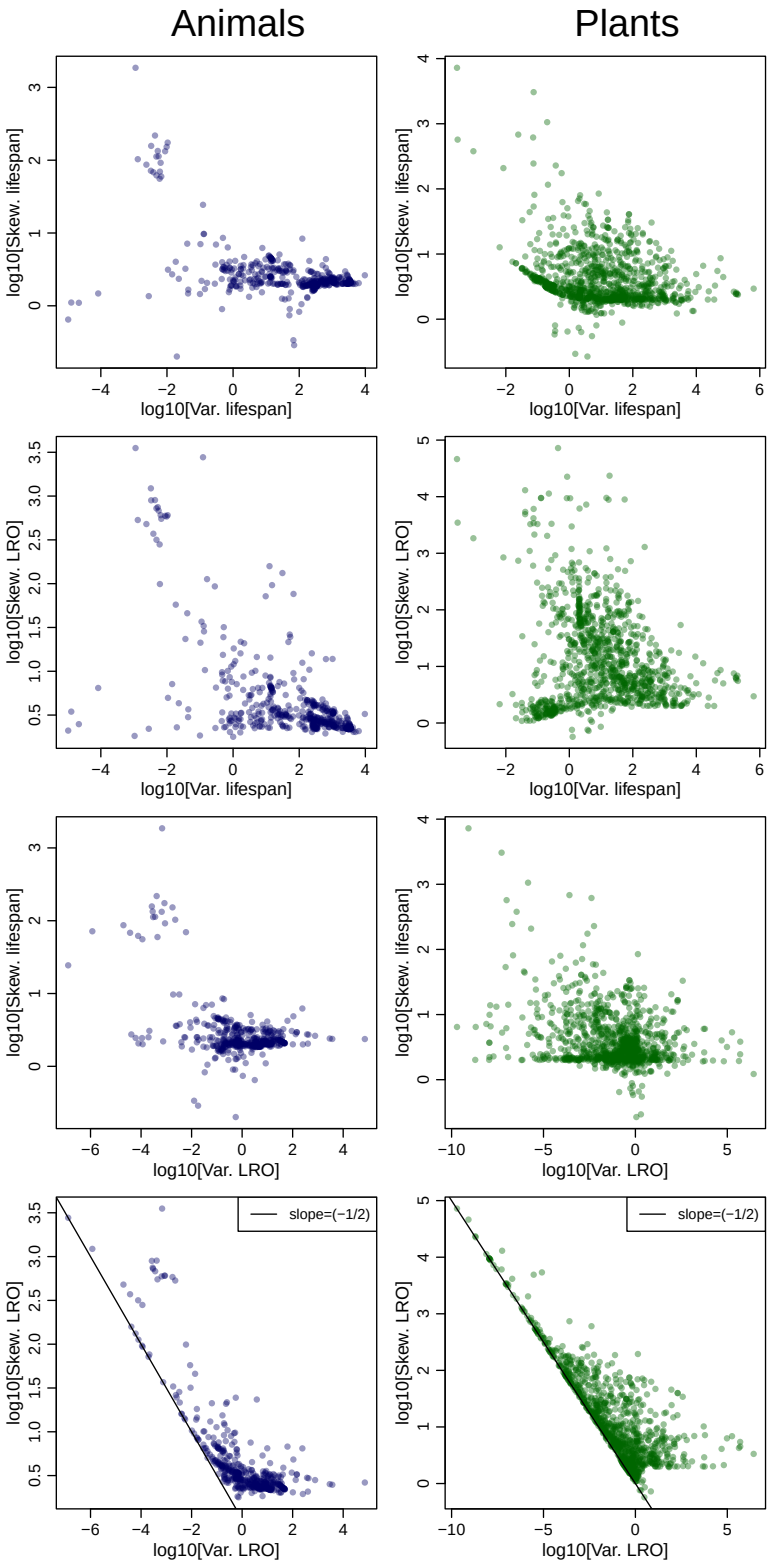

Figure S6: Relationships between measures of skewness and measures of variance, for animals and plants: (first row) lifespan skewness vs. lifespan luck, (second row) LRO skewness vs. lifespan luck, (third row) LRO skewness vs. LRO luck. All of the Kendall's τ correlation coefficients have a corresponding $p < 1e - 10$. Note that the axes are log-scaled.

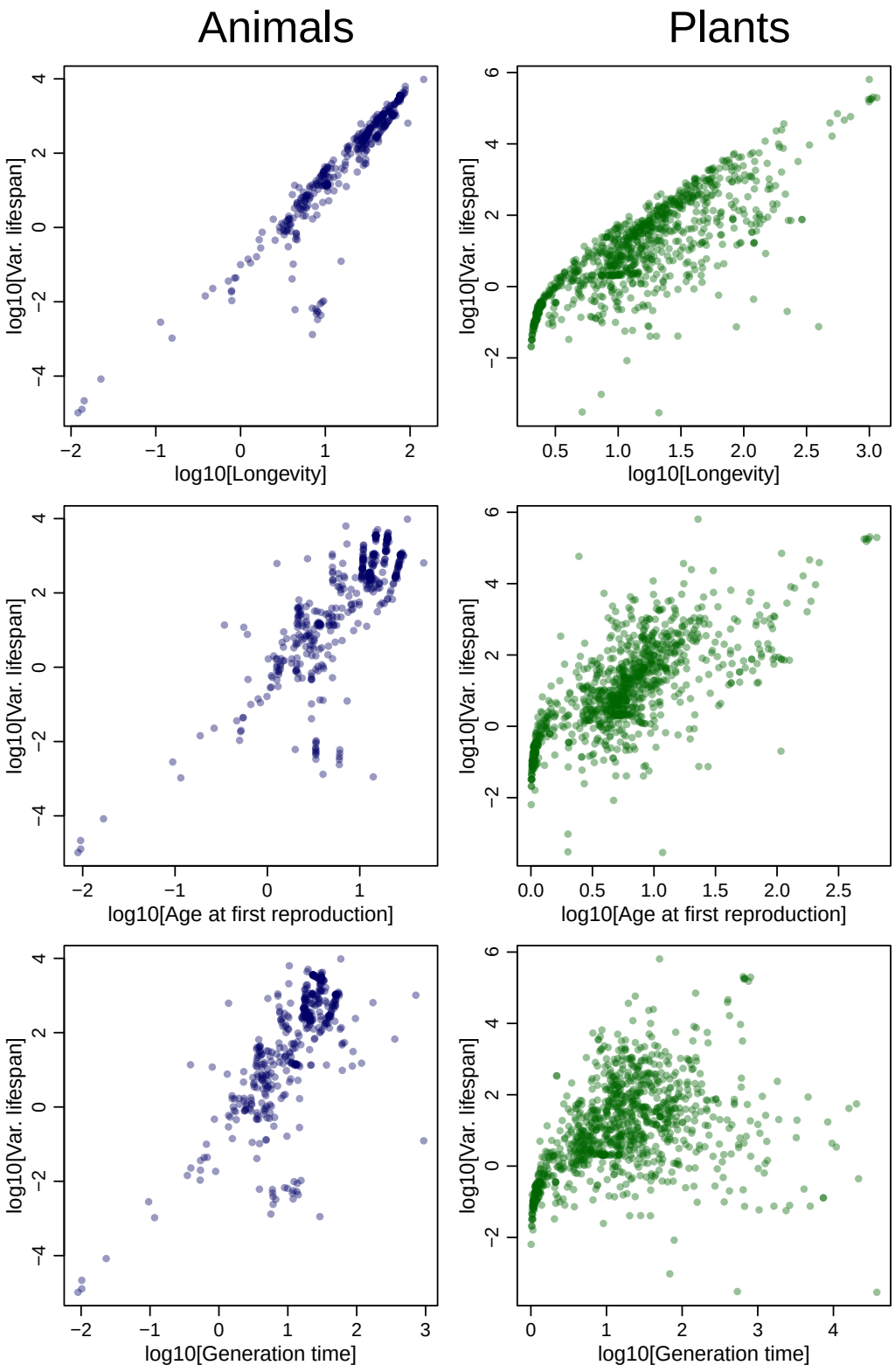

Figure S7: Relationships between lifespan luck and slow life history traits for animals and plants: (first row) expected lifespan of individuals that reproduce at least once, (second row) mean age at first reproduction, and (third row) generation time (T_a). Note that the axes are log-scaled.

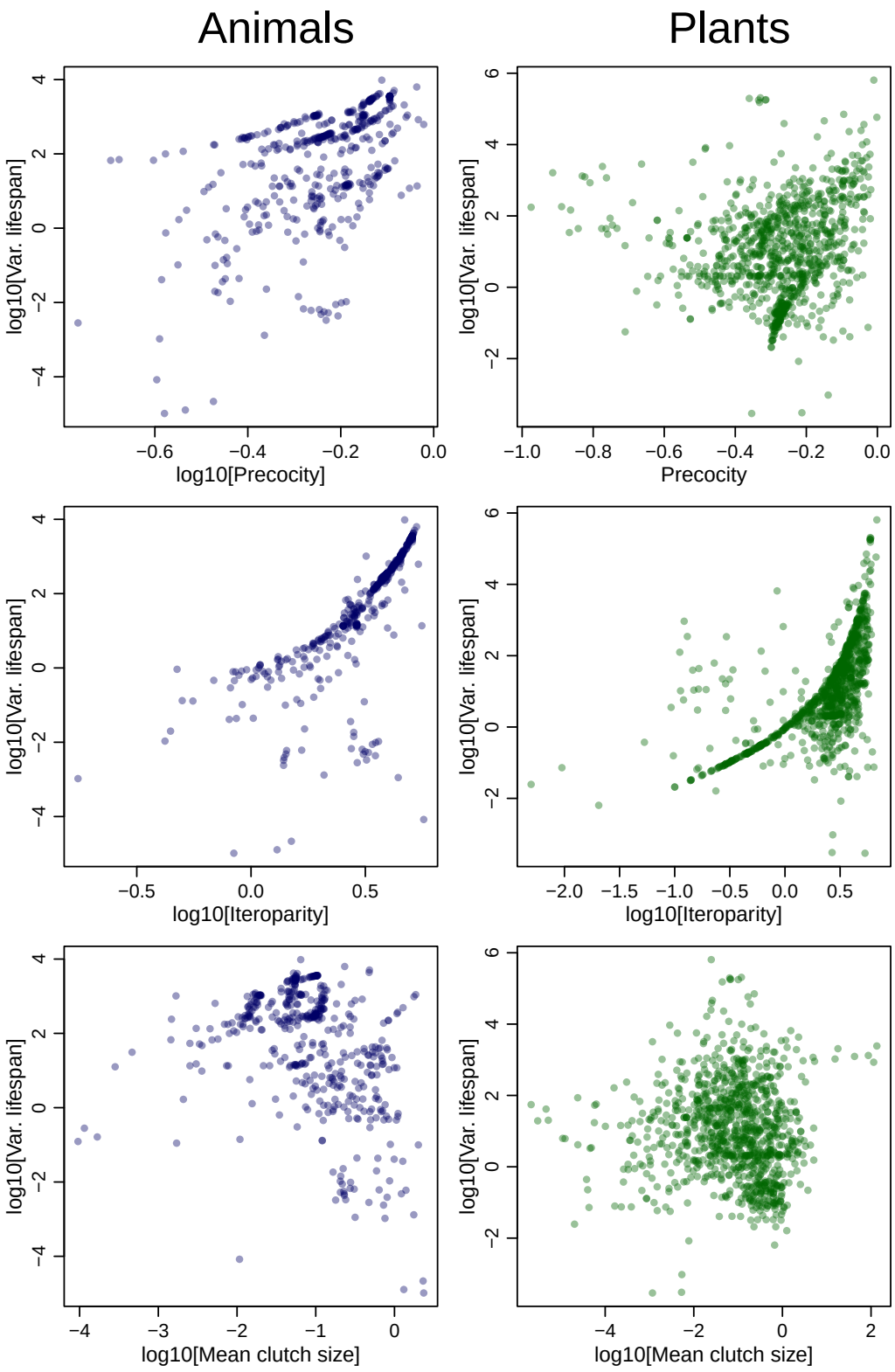

Figure S8: Relationships between lifespan luck and reproductive strategy traits for animals and plants: (first row) precocity, (second row) iteroparity, and (third row) mean clutch size (T_a). Note that the axes are log-scaled.

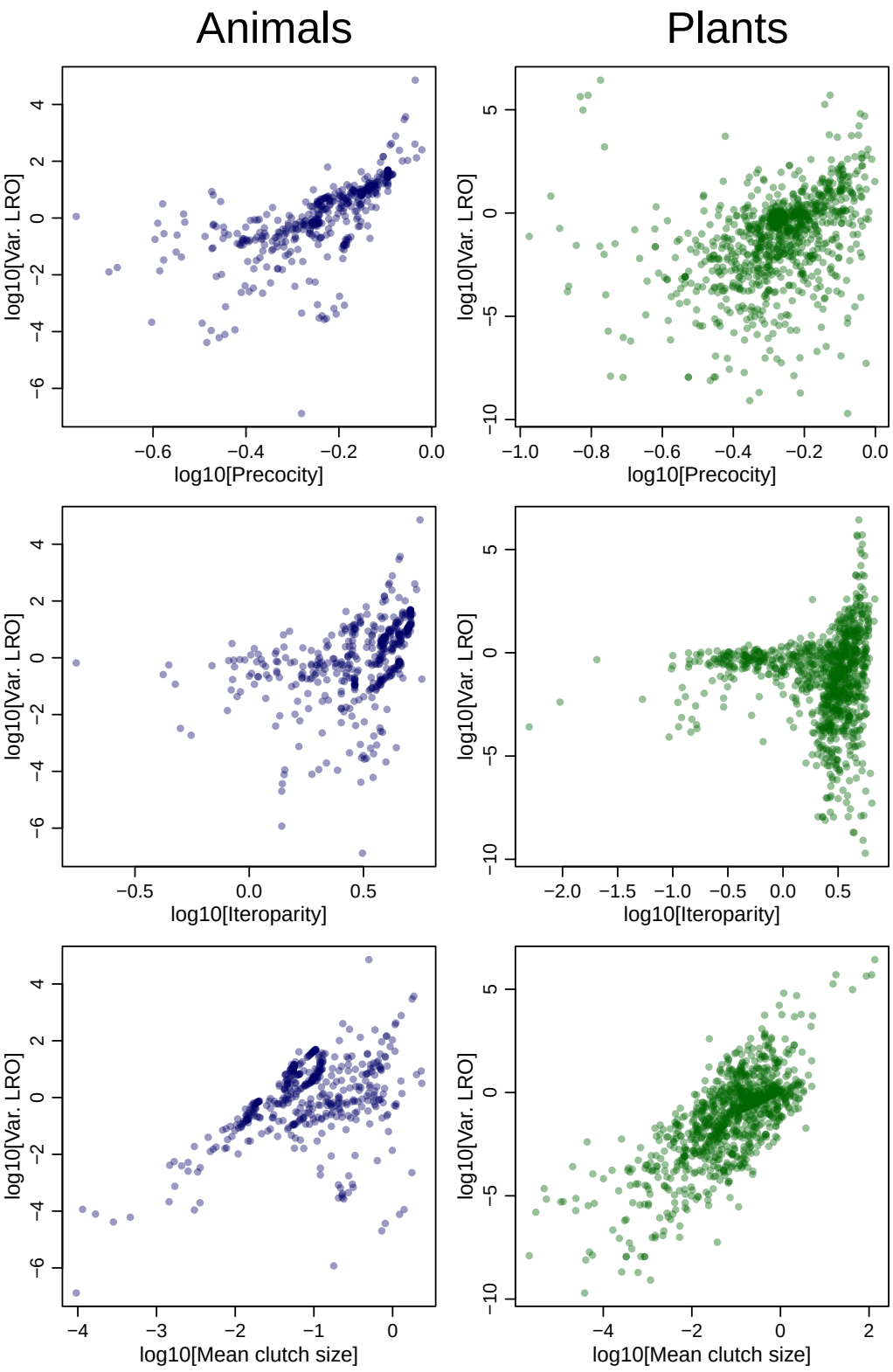

Figure S9: Relationships between LRO luck and reproductive strategy traits for animals and plants: (first row) precocity, (second row) iteroparity, and (third row) mean clutch size (T_a). Note that the axes are log-scaled.

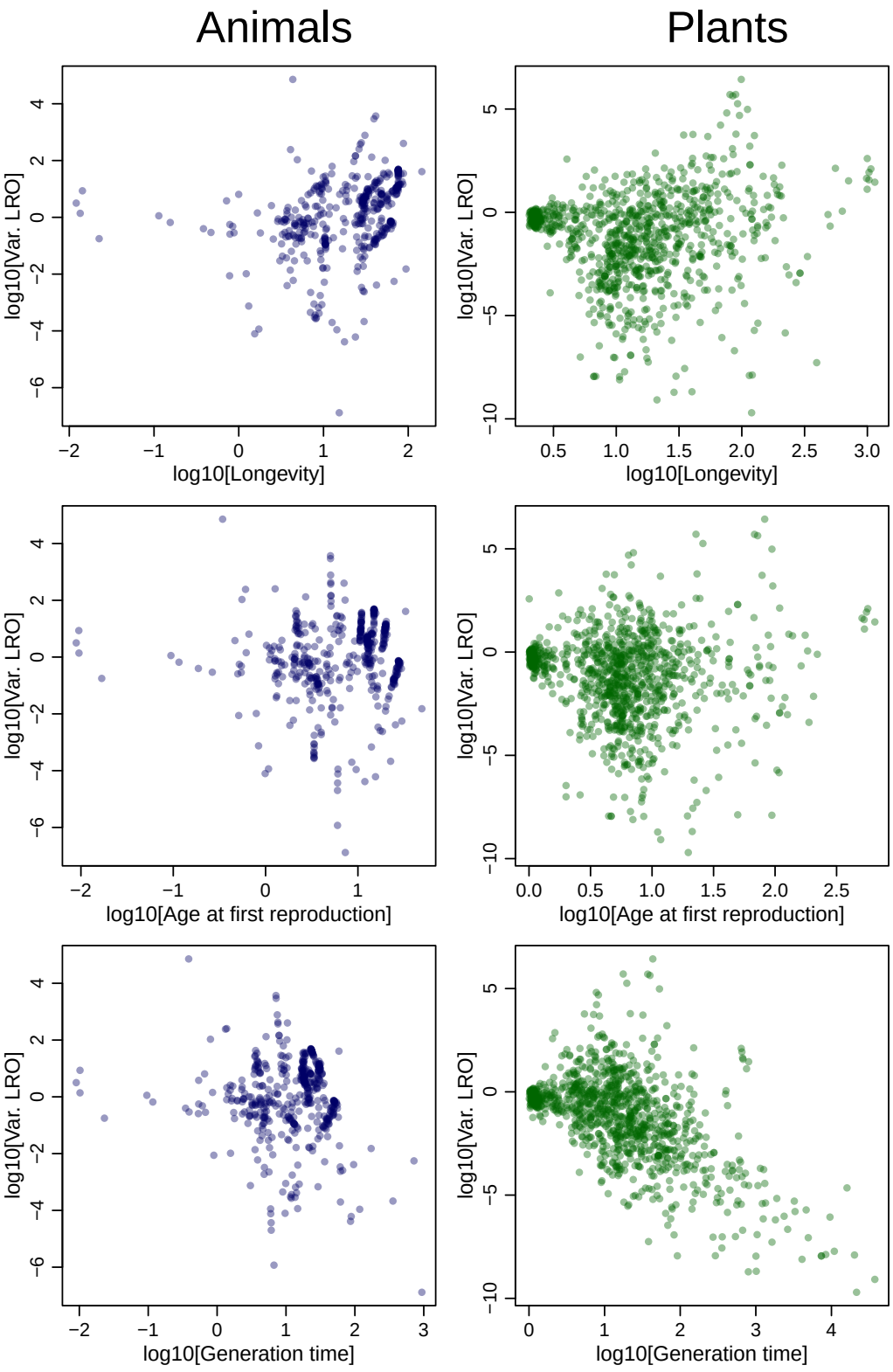

Figure S10: Relationships between LRO luck and slow life history traits for animals and plants: (first row) expected lifespan of individuals that reproduce at least once, (second row) mean age at first reproduction, and (third row) generation time (T_a). Note that the axes are log-scaled.

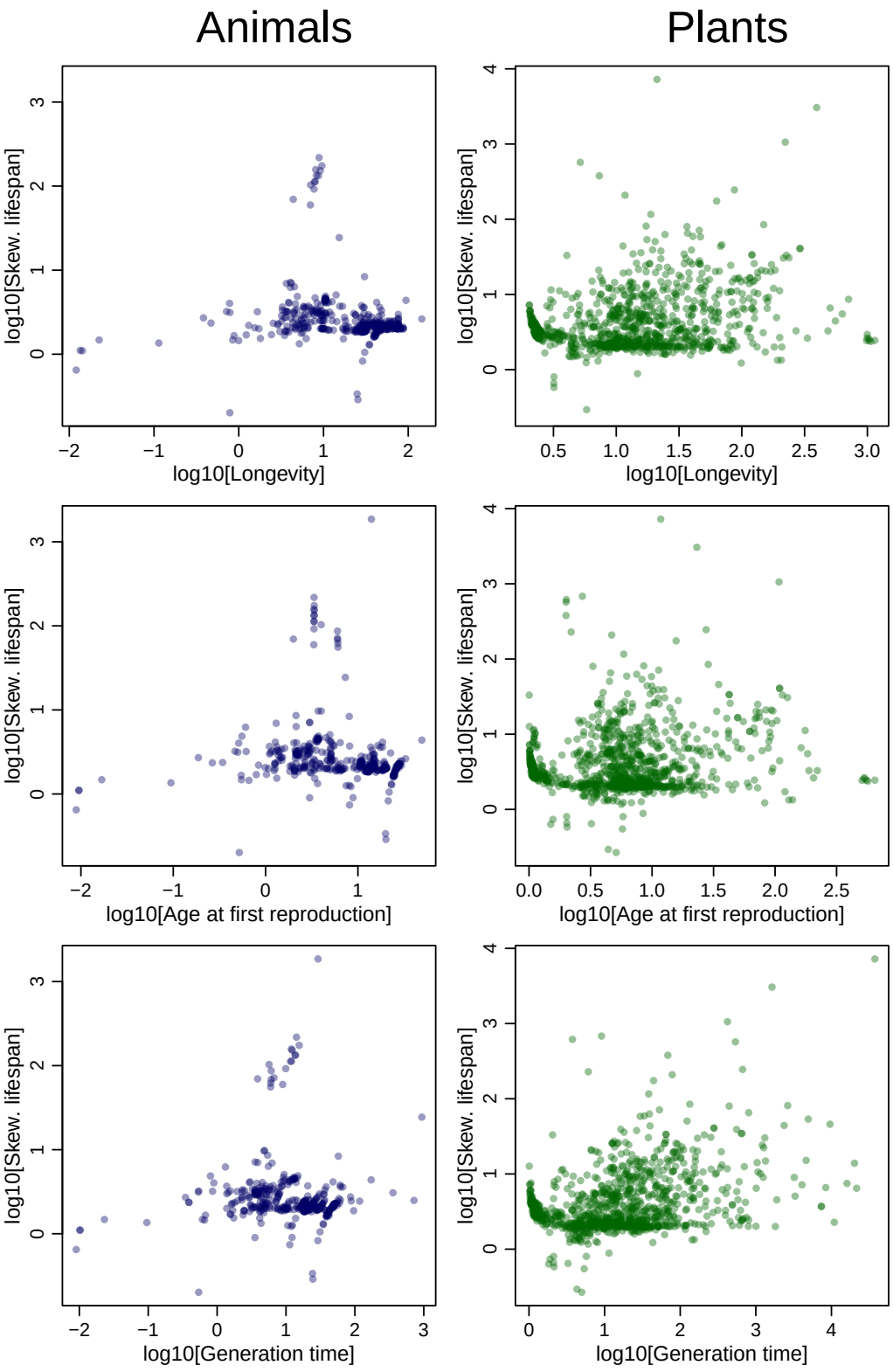

Figure S11: Relationships between lifespan skewness and slow life history traits for animals and plants: (first row) expected lifespan of individuals that reproduce at least once, (second row) mean age at first reproduction, (third row) generation time (T_a). Note that the axes are log-scaled.

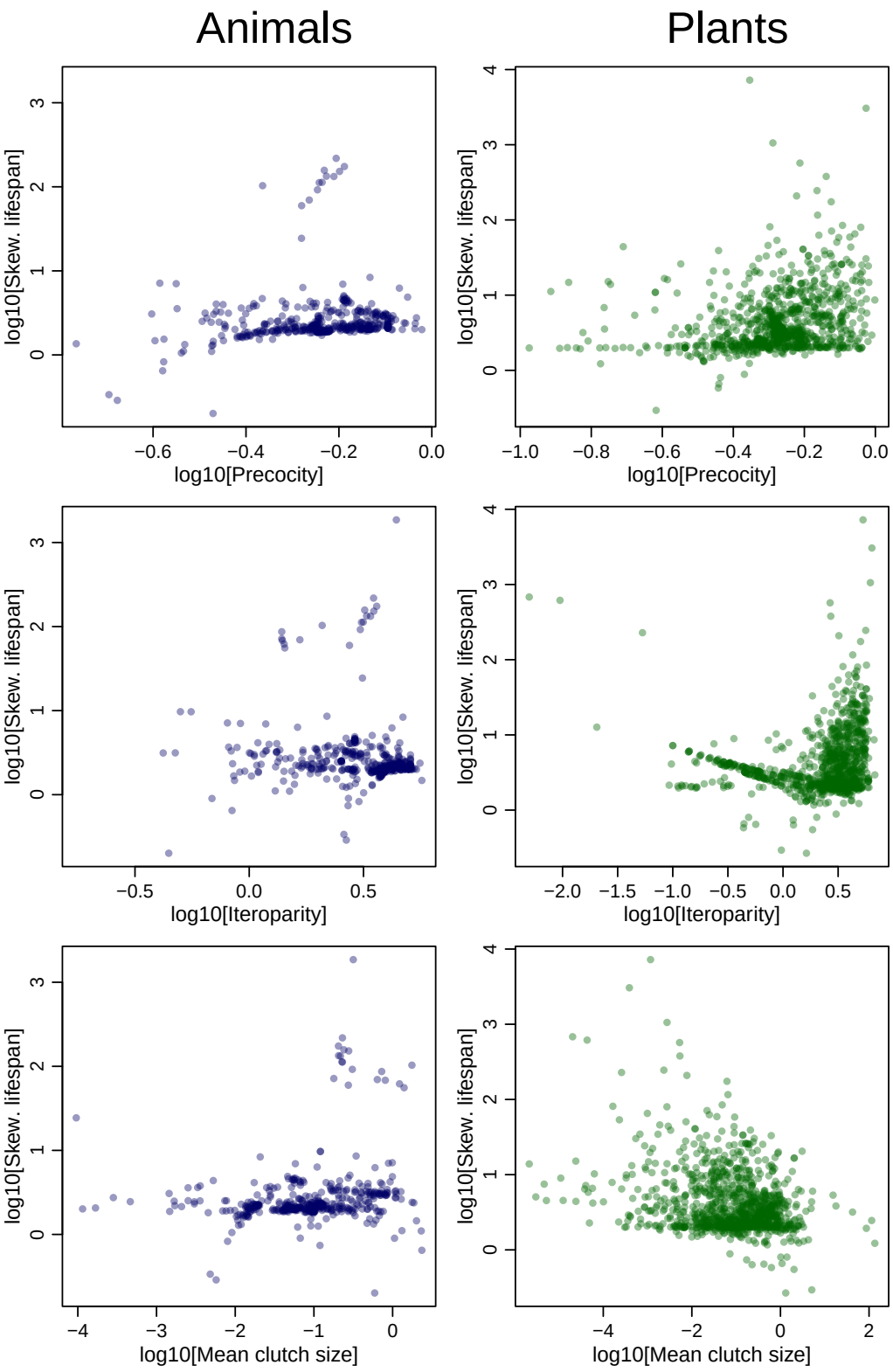

Figure S12: Relationships between lifespan skewness and reproductive strategy traits for animals and plants: (first row) precocity, (second row) iteroparity, (third row) mean clutch size. Note that the axes are log-scaled.

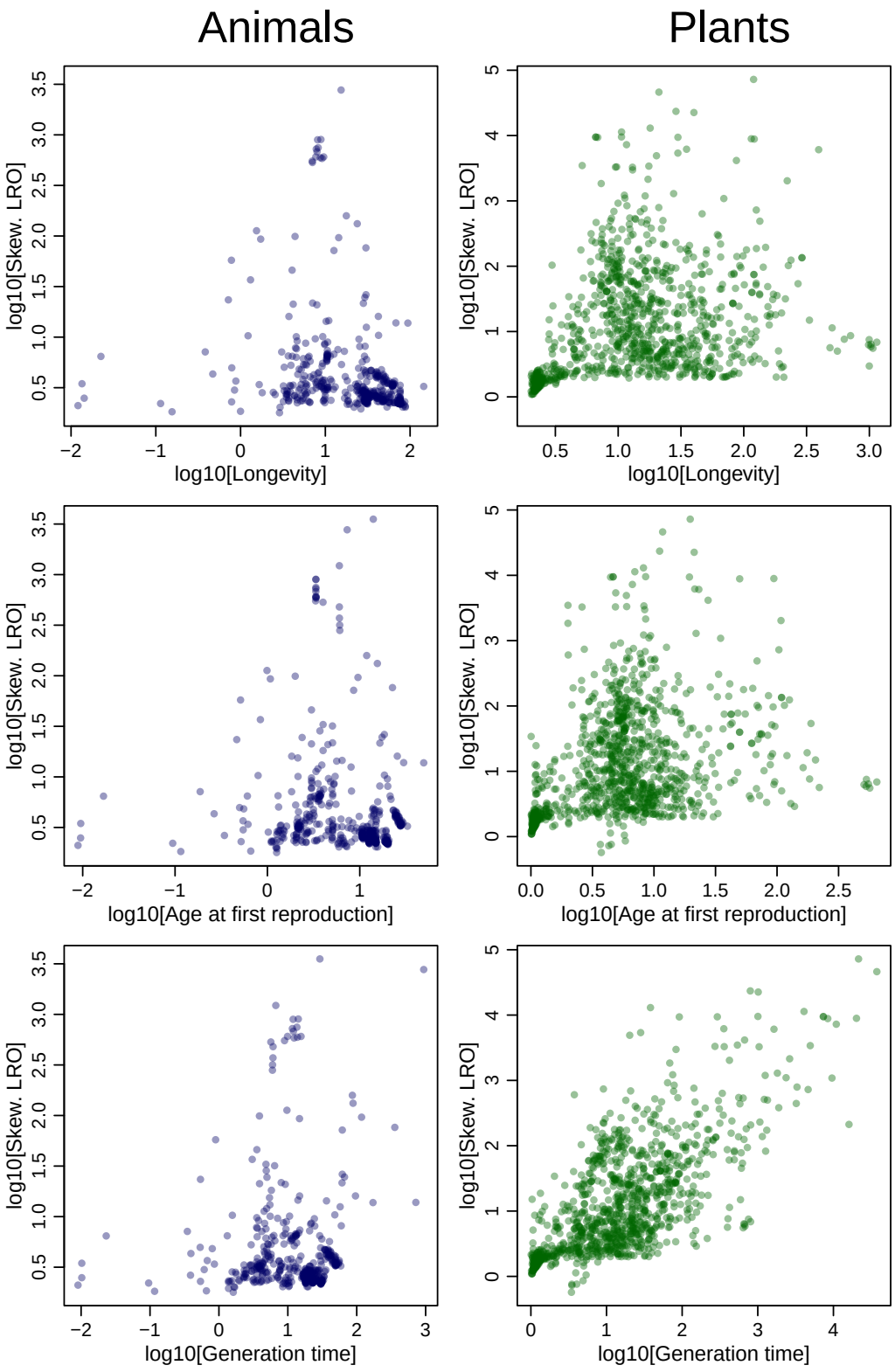

Figure S13: Relationships between LRO skewness and slow life history traits for animals and plants: (first row) expected lifespan of individuals that reproduce at least once, (second row) mean age at first reproduction, (third row) generation time (T_a). Note that the axes are log-scaled.

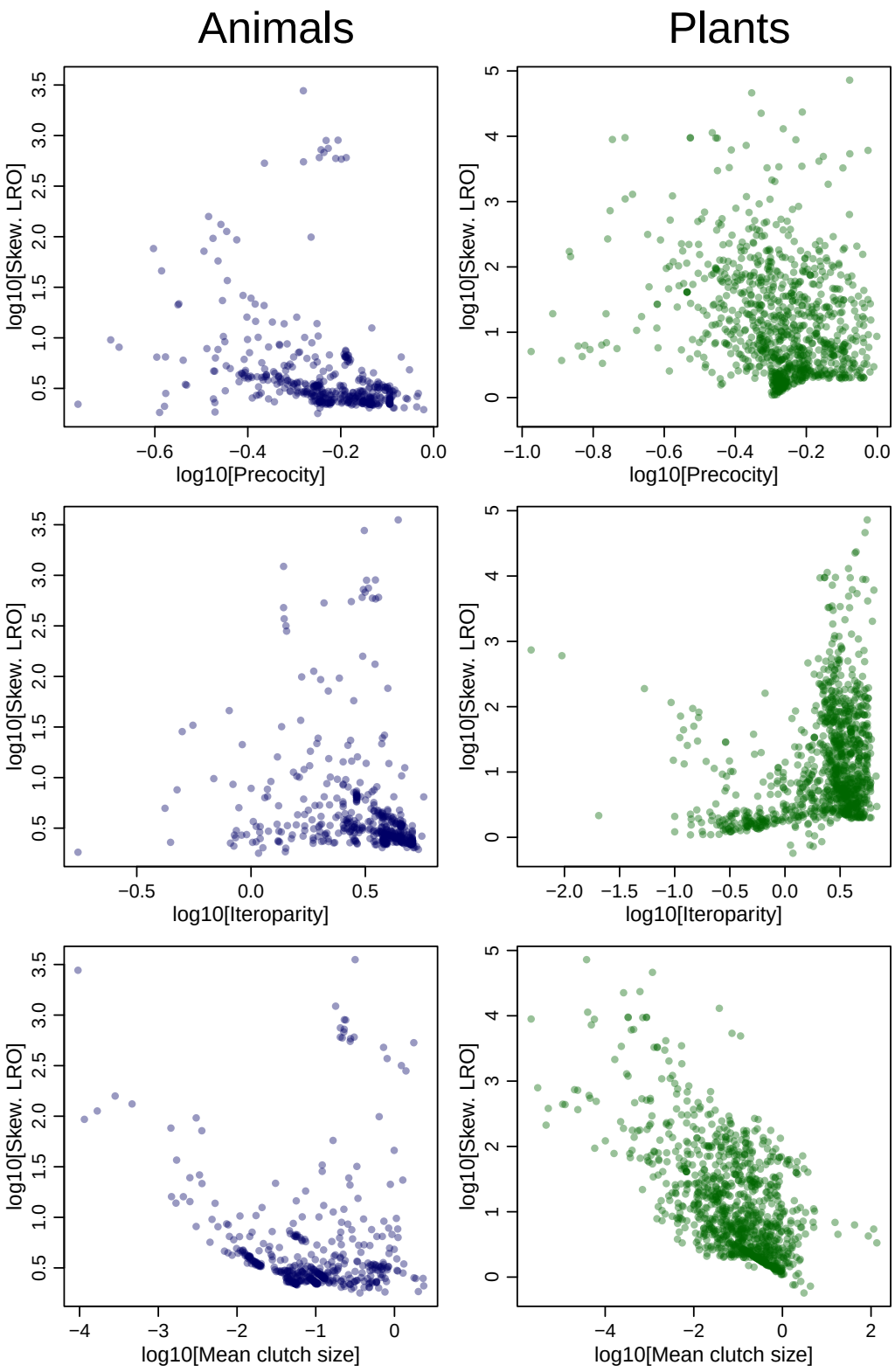

Figure S14: Relationships between LRO skewness and reproductive strategy traits for animals and plants: (first row) precocity, (second row) iteroparity, (third row) mean clutch size. Note that the axes are log-scaled.

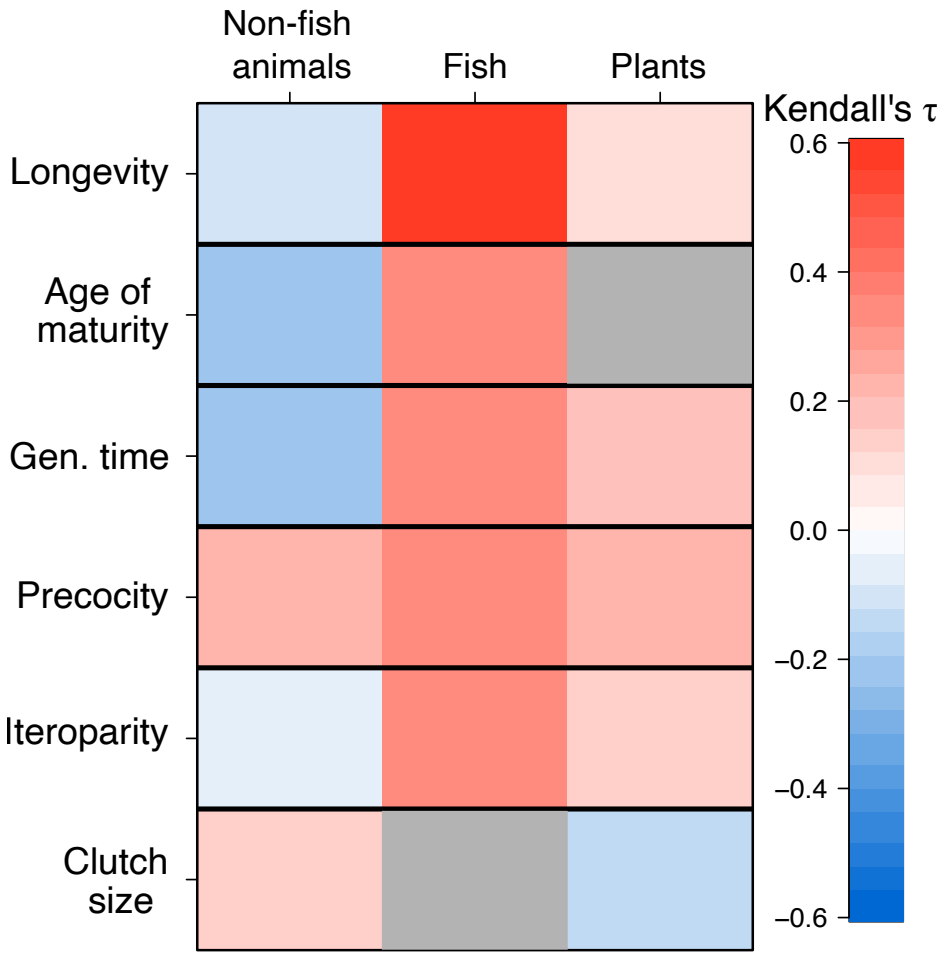

Figure S15: Kendall's τ values for correlations between skewness of lifespan and life history traits for non-fish animals, fish, and plants. Grey squares indicate non-significant ($p > 0.05$) correlations.

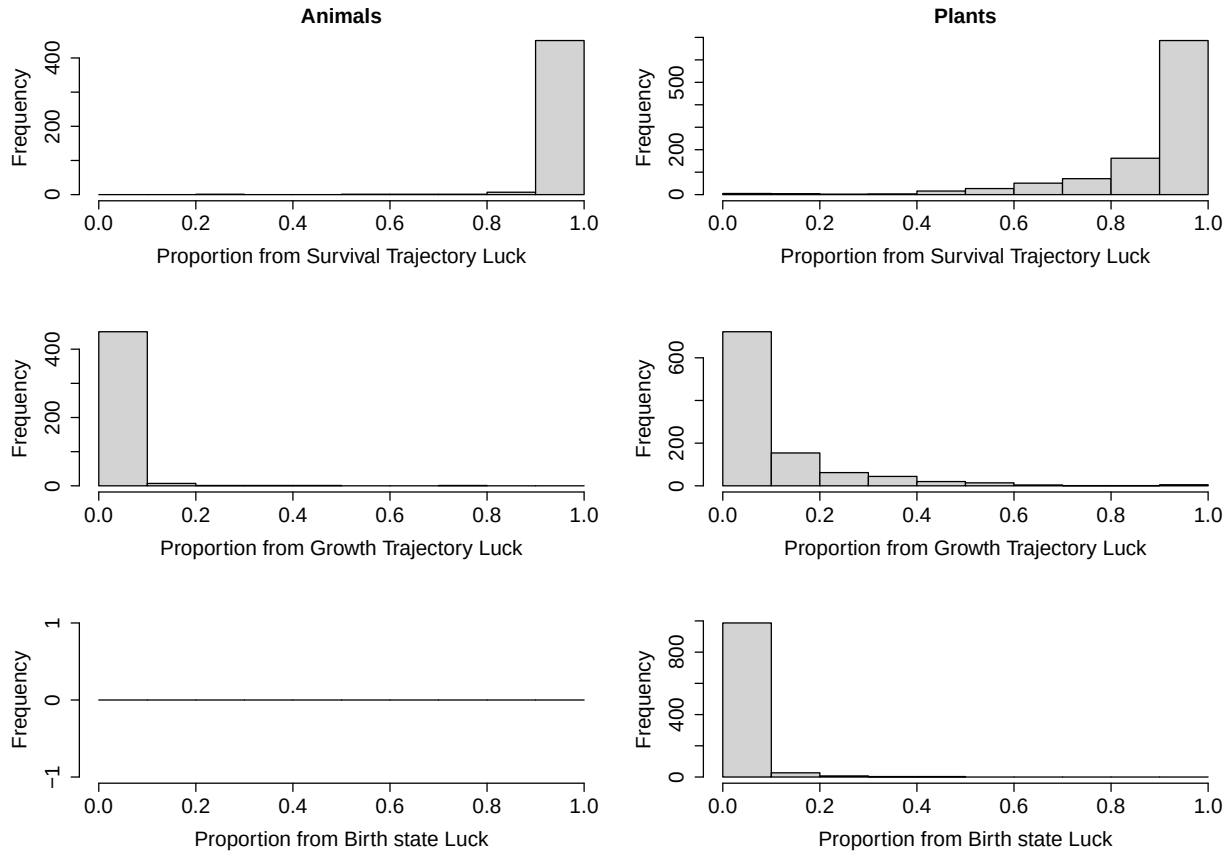

Figure S16: Decomposition of variance in lifespan into contributions from uncertainty in survival, growth, and birth state.

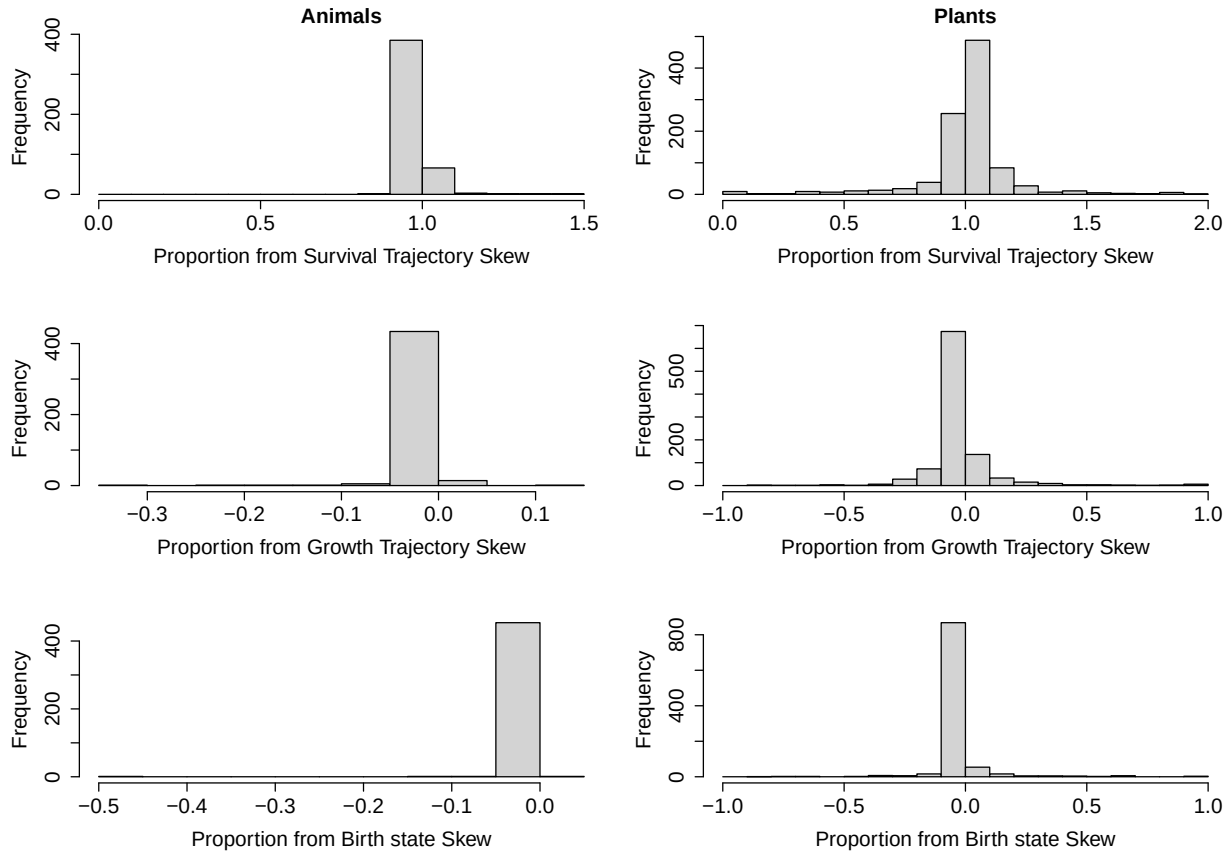

Figure S17: Decomposition of skewness in lifespan into contributions from skewness in survival, growth, and birth state. To aid with visualization in this figure, we excluded 1 model with a ratio of survival trajectory skewness to lifespan skewness greater than 1.5, 20 plant models with a ratio of survival trajectory skewness to lifespan skewness greater than 2, and 8 plant models with a ratio of survival trajectory skewness to lifespan skewness less than 0. Overall, this figure excludes less than 3% of the plant models.